

Air Force Institute of Technology

AFIT Scholar

Theses and Dissertations

Student Graduate Works

3-2003

Effect of Multi-Mode Vibration on Signature Estimation Using a Laser Vibration Sensor

Ngoya Pepela

Follow this and additional works at: <https://scholar.afit.edu/etd>



Part of the [Engineering Physics Commons](#)

Recommended Citation

Pepela, Ngoya, "Effect of Multi-Mode Vibration on Signature Estimation Using a Laser Vibration Sensor" (2003). *Theses and Dissertations*. 4250.

<https://scholar.afit.edu/etd/4250>

This Thesis is brought to you for free and open access by the Student Graduate Works at AFIT Scholar. It has been accepted for inclusion in Theses and Dissertations by an authorized administrator of AFIT Scholar. For more information, please contact richard.mansfield@afit.edu.



**EFFECT OF MULTI-MODE VIBRATION ON SIGNATURE
ESTIMATION USING A LASER VIBRATION SENSOR**

THESIS

Ngoya Pepela, Flight Lieutenant, RAAF
AFIT/GE/ENP/03-02

**DEPARTMENT OF THE AIR FORCE
AIR UNIVERSITY**

AIR FORCE INSTITUTE OF TECHNOLOGY

Wright-Patterson Air Force Base, Ohio

APPROVED FOR PUBLIC RELEASE; DISTRIBUTION UNLIMITED

The views expressed in this thesis are those of the author and do not reflect the official policy or position of either the United States Air Force, United States Department of Defense, United States Government, Royal Australian Air Force, Australian Department of Defence, or Government of the Commonwealth of Australia.

AFIT/GE/ENP/03-02

EFFECT OF MULTI-MODE VIBRATION ON SIGNATURE
ESTIMATION USING A LASER VIBRATION SENSOR

THESIS

Presented to the Faculty

Department of Electrical and Computer Engineering

Graduate School of Engineering and Management

Air Force Institute of Technology

Air University

Air Education and Training Command

in Partial Fulfillment of the Requirements for the

Degree of Master of Science in Electrical Engineering

Ngoya Pepela, BEng *Flinders University of South Australia*

Flight Lieutenant, RAAF

March, 2003

APPROVED FOR PUBLIC RELEASE; DISTRIBUTION UNLIMITED

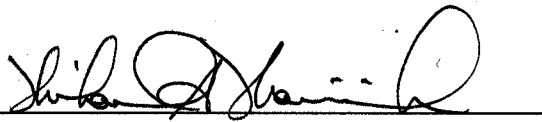
AFIT/GE/ENP/03-02

EFFECT OF MULTI-MODE VIBRATION ON SIGNATURE
ESTIMATION USING A LASER VIBRATION SENSOR

Ngoya Pepela, BEng *Flinders University of South Australia*

Flight Lieutenant, RAAF

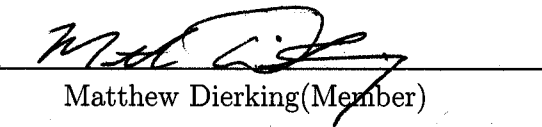
Approved:



Michael A. Marciniak (Chairman)

13 Mar 03

date



Matthew Dierking (Member)

3/17/03

date



Richard Cobb (Member)

14 MAR 03

date

Acknowledgements

My sincerest thanks to my thesis advisor, Lt Col Michael Marciniak. I am grateful for both the technical and administrative support he provided to me, as well as the latitude and opportunity he extended while I tackled this endeavor. With your open door policy I was always able to consult you with all aspects of my thesis.

I would also like to thank the rest of my committee members. Mathew Dierking from the Air Force Research Laboratories, thank you for providing me with an interesting thesis topic and advice along the way on how to tackle this undertaking. Major Richard Cobb, you were a God send. You willingly joined my thesis committee, and provided me with many of the missing puzzle pieces that helped me to consolidate everything.

I am also grateful to both the Royal Australian Air Force, and the United States Air Force for the opportunity that was provided to me to undertake this course.

Last but by no means least, I would like to thank my mother for the encouragement she has provided me throughout my life leading me to where I am now.

Ngoya Pepela

Table of Contents

	Page
Acknowledgements	iv
List of Figures	ix
List of Tables	xiv
List of Abbreviations	xv
Abstract	xvi
I. Introduction	1-1
1.1 Research Motivation	1-1
1.2 Research Goals	1-2
1.3 Thesis Organization	1-2
II. Background	2-1
2.1 Introduction	2-1
2.2 Target Discrimination Using Laser Vibration Sensing	2-1
2.3 Laser Vibration Sensor (LVS) Theory	2-1
2.4 Multi-Mode Vibration	2-3
2.5 Modal Analysis	2-4
2.6 Target Selection Considerations	2-4
2.6.1 Temperature Fluctuations	2-4
2.6.2 Complexity of Modal Structure	2-4
2.6.3 Clamped-Free versus Clamped-Clamped Beam	2-5
2.6.4 Surface Treatment	2-5
2.7 Signal and Waveform Analysis	2-6
2.8 Laser Beam Propagation	2-6

	Page
III. Experiment	3-1
3.1 Introduction	3-1
3.2 Aim	3-1
3.2.1 Multi-Mode Vibration	3-1
3.2.2 Frequency Spectrum Estimation	3-1
3.3 Equipment Setup Description and Settings	3-1
3.3.1 Laptop Settings	3-2
3.3.2 LVS Settings	3-3
3.3.3 Laser Beam	3-3
3.3.4 Signal Generator and Amplifier	3-3
3.4 Clamped-Clamped Beam as a Target	3-3
3.4.1 Target Surface	3-4
3.4.2 Theoretical Modal Analysis of Eigenfrequencies of Target	3-4
3.4.3 Practical Modal Analysis of Eigenfrequencies of Target	3-5
3.5 Modeling Experiment	3-8
3.5.1 Assumptions and Simplifications	3-9
3.6 Experimental Procedures	3-11
3.6.1 Practical Observation of Multi-Modal Effects	3-11
3.6.2 Use of Model to Observe Multi-Modal Effects	3-11
IV. Results and Analysis	4-1
4.1 Introduction	4-1
4.2 Experimental Results	4-1
4.2.1 Expanded Beam Over Node at 2058 Hz	4-1
4.2.2 Expanded Beam Over Nodes at 1460 Hz and 996 Hz	4-1

	Page
4.2.3 Expanded Beam Over Node at 585 Hz	4-3
4.3 Simulation with MATLAB® model Experiment Results	4-4
4.4 Peak PSD as LVS is Moved Away from Node	4-5
4.5 Experimental Conclusions	4-6
V. Mitigating Spectral Elimination	5-1
5.1 Introduction	5-1
5.2 Target Measurement using Continuous Scanning Techniques	5-1
5.2.1 Theory	5-1
5.2.2 Experimental Scanning Laser Across Nodes	5-1
5.2.3 Results and Conclusions of Continuous Scanning Techniques	5-2
5.3 Laser Blocking at Source	5-3
5.3.1 Theory	5-3
5.3.2 Laser Blocking Experiment	5-4
5.3.3 Conclusion	5-5
5.4 Signal Processing Techniques Discussion	5-5
VI. Conclusions and Recommendations	6-1
6.1 Restatement of Research Goal	6-1
6.2 Conclusion	6-1
6.2.1 Multi-Modal Impact on Signature Estimation	6-1
6.2.2 Mitigation of Multi-Modal Impacts	6-1
6.3 Recommendations	6-2
Appendix A. Examples of Modes of Vibration of a circular Membrane taken from [25]	A-1
Appendix B. Equipment List	B-1

	Page
Appendix C. File Format 1011 - AFRL (John Schmoll)	C-1
Appendix D. Modal Analysis - MATLAB® code	D-1
Appendix E. Modeling of Clamped-Clamped Beam - MATLAB® Code	E-1
Bibliography	BIB-1

List of Figures

Figure		Page
2.1.	Michleson arrangement used to measure vibrations [24].	2-2
2.2.	String displaying two different modes of vibration.	2-3
2.3.	Horizontal displacement of points on a clamped-free beam are larger than on a clamped-clamped beam. This can lead to errors. For example in (a), if a sample is taken when the clamped-free beam is in the horizontal position then the point 'X' may not be seen by the laser.	2-5
2.4.	Beam Expander - An expanded beam with collimation maintained.	2-7
3.1.	General set-up of experiment.	3-2
3.2.	Plots of the first six modes shapes with the amplitude arbitrarily normalized for display purposes.	3-7
3.3.	Beam showing points where LVS measured the surface velocities.	3-8
3.4.	Spatial frequencies on clamped-clamped beam observed at 1469 Hz. The darker shaded areas are indicative of nodal points and are not moving with respect to the 1469 Hz signal.	3-8
3.5.	Some of the spatial frequencies identified on the randomly excited clamped-clamped beam.	3-9
3.6.	Section of clamped-clamped beam showing points where vertical nodes at 996 Hz and 2058 Hz have been identified.	3-10
4.1.	Expanded beam illuminating node at 2058 Hz and associated PSD. Notice the near annihilation in the 2058 Hz spectral line power.	4-2
4.2.	Expanded beam partially blocked illuminating only one side of node at 2058 Hz and associated PSD. Notice the strong return of the spectral line at 2058 Hz.	4-2

Figure		Page
4.3.	Expanded beam illuminating node at 1460 Hz and associated PSD. Notice the peak at 1460 Hz has a small magnitude in comparison to the other eigenfrequencies of the beam.	4-3
4.4.	Expanded beam partially blocked illuminating one side of node at 1460 Hz and associated PSD. Notice the strong return of power in the signal at 1460 Hz. This is a nodal point for the 2700 Hz signal which explains why it is missing from the PSD.	4-3
4.5.	Expanded beam illuminating node at 996 Hz and associated PSD. Again the spectral line at 996 Hz is almost non-existent	4-4
4.6.	Expanded beam partially blocked illuminating one side of node at 996 Hz and associated PSD. Notice the rise in power of the spectral line at 996 Hz.	4-4
4.7.	True PSD of clamped-clamped beam showing all six eigenfrequencies programmed into the beam.	4-5
4.8.	PSD of Simulated LVS illuminating node common to mode 2 (308 Hz), mode 4 (1001 Hz) and Mode 6 (2088 Hz). Notice all three frequencies are missing from the PSD.	4-6
4.9.	PSD of Simulated LVS laser spot centered around node at 605 Hz.	4-7
4.10.	PSD of Simulated LVS laser spot centered around node at 1495 Hz.	4-7
4.11.	PSD of target as laser is moved in 0.001 m increments away from washout condition at the node common to frequencies 605 Hz, 1001 Hz and 2088 Hz. This Figure shows the first four incremental moves.	4-8
4.12.	Peak spectral PSD for spectral lines at 608 Hz, 1001 Hz and 2088 Hz as the simulated LVS is moved away in 0.001 increments away from washout condition. This Figure shows the first nine incremental movements. This result is specific to the set-up used to conduct this experiment.	4-9

Figure		Page
5.1.	Scanning across a 996 Hz node. (a) Position of laser on target at beginning of scan and (b) position of laser on target at end of scan.	5-2
5.2.	PSD showing 996 Hz peak observed while scanning across the node.	5-3
5.3.	(a) Circular aperture and (b) its Fourier transform.	5-4
5.4.	(a) Half of a circular aperture and (b) its Fourier transform.	5-4
5.5.	PSD showing the rise in spectral line at 2058 Hz and 996 Hz when the intensity pattern is changed by half blocking the laser.	5-5
A.1.	The (0,1) Mode. The mode number is designated as (0,1) since there are no nodal diameters, but one circular node (the outside edge). A node is a point (or line) on a structure that does not move while the rest of the structure is vibrating. The (0,1) mode of a drum, is excited when the drum head is struck at its center. When vibrating in this mode the membrane acts much like a monopole source, which radiates sound very effectively. Since it radiates sound so well when vibrating in this manner, the membrane quickly transfers its vibrational energy into radiated sound energy and the vibration dies away. The short duration (fraction of a second) of the (0,1) mode means that this mode does not contribute greatly to the musical tone quality of a drum. In fact, when struck at the center a tympani, or other large drum, produces a "thump" which decays quickly and with no definite pitch.	A-1

- A.2. The next mode is the (1,1) with one nodal diameter and one circular node (the outside edge). The exact location of the nodal diameter depends on the homogeneity of the membrane and the initial conditions when the vibration starts. The frequency of the (1,1) mode is 1.593 times the frequency of the (0,1) mode. When vibrating in the (1,1) mode a circular membrane acts much like a dipole source; instead of pushing air away from the membrane like the (0,1) mode does, in the (1,1) mode one half of the membrane pushes air up while the other half sucks air down resulting in air being pushed back and forth from side to side. As a result, the (1,1) mode radiates sound less effectively than the (0,1) mode which means that it does not transfer its vibrational energy into radiated sound energy as quickly as the (0,1) mode and therefore, the (1,1) mode takes longer to decay. Because the (1,1) mode "rings" for a while, it contributes to the musical sound or pitch of a drum. When a tympani, or other large drum, is struck somewhere between the center and outer edge, the sound has a definite pitch which lingers for a several seconds. A-2
- A.3. The (0,2) mode, shown above does not have any diameter nodes, but has two circular nodes - one at the outside edge and one at a distance of 0.436 a (a is the radius of the circular membrane) from the outer edge. The frequency of the (0,2) mode is 2.295 times the frequency of the (0,1) mode. Like the (0,1) mode, the (0,2) mode is excited when the membrane is struck at the center. The sound radiation characteristics of the (0,2) mode are more complicated than the first three modes - it appears to be a mix between a monopole and a dipole. Its decay time is longer than the (0,1) mode, but shorter than the (1,1) mode. As a result, it contributes to the "thump" sound when a drum is hit at the center, but does not contribute much to the musical pitch of a drum when A-3

Figure		Page
A.4.	The (1,2) mode has one nodal diameter and two nodal circles. The frequency of the (1,2) mode is 2.917 times the frequency of the (0,1) mode. As you might expect after looking at the first several modes of the circular membrane, the (1,2) mode does not radiate sound very effectively. It has somewhat of a quadrupole type behavior. Thus, the (1,2) mode takes a relatively long time to decay. However, this mode doesn't seem to play a dominant role in the musical tone quality of a drum.	A-4
B.1.	Clamped-clamped beam fixed at both ends with a high reflectance diffuse coating. The clamped-clamped beam has a piezoelectric transducer used to excite it located on the back.	B-1
B.2.	Amplifier.	B-2
B.3.	Collimation Tester.	B-2
B.4.	Polytech OFV-3001 Controller(top) and Onisoki FFT Analyzer with Signal Generator(bottom).	B-3
B.5.	Polytech Sensor Head OFV-353 and Beam Expander (Behind Sensor Head). The Laser Leaves the Sensor Head, gets reflected off two Mirrors into the Beam Expander. The Elevation and Azimuth of Directed Laser Energy is Controlled by Motors that Control the Plate on Which The Sensor Head and Beam Expander Sit. The Motors are Controlled by Laptop Software. .	B-3
B.6.	Laptop Contains Software Developed by AFRL that Controls Both the Position of Directed Laser Energy and Records Information in File Format "1011" as is Shown in Appendix C. . .	B-4
B.7.	Equipment Set Up to Take Readings.	B-4

List of Tables

Table		Page
3.1.	Sampling Settings.	3-3
3.2.	LVS Settings.	3-3
3.3.	Physical properties of beam.	3-4
3.4.	First six values of $\lambda_n l$	3-5
3.5.	Calculated eigenfrequencies ω_n of beam.	3-6

List of Abbreviations

Abbreviation	Page
Laser Vibrations Sensor LVS	1-1
Non-Cooperative Identification NCID	2-1
power spectral densities PSD	2-6
Fast Fourier Transform FFT	5-5

Abstract

A Laser Vibrations Sensor (LVS) can be used to determine the vibrational spectrum of targets, such as vehicles, using heterodyne laser Doppler velocimetry. The vibrational spectra of vehicles are known to have characteristic resonances due to the motors, gears and other moving parts. Each particular class of vehicle has a unique vibrational spectrum. This research shows of how a body vibrating in higher order modes has the opportunity to eliminate spectral content of the target's vibrational spectrum while using an LVS to perform spectrum estimation. This is due to roughly equal amounts of laser photons with equal and opposite information about the target's velocity returning from the body under investigation. This is especially so when observing targets at large distances, and the laser spot size has increased to encapsulate higher order modes that are vibrating with frequencies that are used for identification purposes. The research also contains preliminary investigations into the mitigation of these effects by use of laser scanning, laser pattern intensity changes and advanced signal processing techniques.

EFFECT OF MULTI-MODE VIBRATION ON SIGNATURE ESTIMATION USING A LASER VIBRATIONS SENSOR

I. Introduction

Vibrational signature is a powerful target discriminator capable of providing positive identification of targets such as ships, aircraft and land vehicles. A Laser Vibrations Sensor (LVS) , also commonly known as a laser vibrometer, can be used to remotely obtain vibrational signatures. Vibration sensing via LVS is based on the modulation of incident radar laser beam by mechanical displacements associated with machine vibrations [15].

There are a number of anomalies that are observed in the field when trying to identify targets using an LVS. It is postulated that one of these anomalies is caused by multi-modal vibrations.

While operating an LVS over large distances, the spot size¹ of the laser increases so that it illuminates a large section of the target. The illuminated area thus encapsulates many nodes and anti-nodes on the target. These nodes and anti-nodes may belong to modes that are vibrating at frequencies used in the identification of the target². This thesis examines if the multi-mode vibrations on the target can affect the signature estimation process.

1.1 Research Motivation

Knowing the effects of multi-mode vibrations on the signature estimation process will potentially provide insight into methods of how to improve target iden-

¹Diameter of the laser beam

²See section 2.4 for a description of modes, nodes and anti-nodes

tification and accuracy. This has openings in many areas of defence, as well as commercially. In the battle field, this has applications in the reduction of friendly fire, as well as improved adversary identification. In the commercial world, the LVS is used in a number of areas including but not limited to:

1. Damage detection of both micro (*e.g.* Micro Electro Mechanical System (MEMs) devices) and macro (*e.g.* bridges and buildings) structures [5].
2. Medical applications[22].
3. Mode shape prediction[28].

1.2 Research Goals

1. Determine if multi-mode vibrations can eliminate spectral line content from the vibrational spectrum of a target when using an LVS.
2. Perform preliminary investigations into methods of mitigating any negative effects caused by multi-mode vibrations during the spectrum estimation process.

1.3 Thesis Organization

Chapter I introduces the problem that is to be examined. Chapter II provides the background material required to give the reader an understanding of the work covered. A literature review covering related topics is also presented. Chapter III describes the experiment conducted to achieve the first goal as outlined in Section 1.2. The results that were obtained are reported and analyzed in Chapter IV. Based on the results obtained, Chapter V provides preliminary research into methods that could be investigated further to mitigate the effects of multi-mode vibrations. Chapter VI restates the thesis goal, summarizes research findings and offers recommendations for future research.

II. Background

2.1 Introduction

This chapter introduces background theory. No literature was found specifically on the effects of multi-mode vibrations on vibration sensing. However, current literature relevant to the experiment conducted and the equipment used is also introduced.

2.2 Target Discrimination Using Laser Vibration Sensing

The vibrational spectra of the exterior skin of vehicles are known to have characteristic resonances due to the physical structure excited by the resonances of the motors, gears and other moving parts. A particular class of vehicle may have a unique vibrational spectrum that can be exploited for Non-Cooperative Identification (NCID) purposes [15].

Target vibrational spectrum estimation via laser vibration sensing has been shown to be a powerful method of classifying targets. There are numerous papers of theoretical and practical results demonstrating the ability of laser vibration sensing to discriminate between targets. For example, [17] shows how vibration sensing can be used to identify helicopters and [1] uses vibration sensing to discriminate between different motor vehicles.

2.3 Laser Vibration Sensor (LVS) Theory

The Laser Vibration Sensor used for this thesis is a Polytech OFV-3001 as described in [23]. A description of LVS basics can be found in [24]. LVS theory is summarized here for ease of accessibility.

The LVS is based on the Doppler effect. There are numerous texts describing the workings of laser Doppler radar including [23].

A laser of frequency, f_o , is focused onto the object under investigation. The frequency, f_{mod} , of the light scattered back is determined by the object's instantaneous velocity. The difference between these two frequencies is the Doppler frequency, f_D .

To determine the difference in frequencies, a Michelson-type arrangement as shown in Figure 2.1 is used. In this set-up, the laser-beam is sent through a beam splitter, whereby part of the signal is directed to a reference mirror, and the other to the target. Upon reflection from the target, the signal interferes with the reference signal producing a beat frequency which can be measured at the photodetector by calculating the rate of change of interference fringes. Further information on interference can be found in [11].

Once f_D is determined, the instantaneous velocity can be determined by the well known Doppler equation[24]:

$$f_D = \frac{2v}{\lambda} \quad (2.1)$$

where v is the instantaneous velocity of the object under investigation, and λ is the wavelength of the laser used.

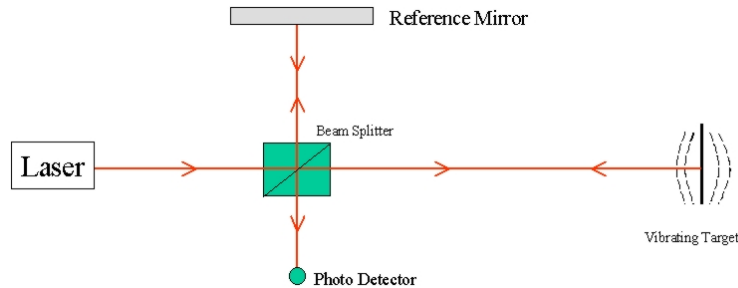


Figure 2.1. Michleson arrangement used to measure vibrations [24].

The photodetector thus outputs a voltage signal that is proportional to the velocity of the target. The voltage signal can then be analyzed for frequency content.

2.4 Multi-Mode Vibration

Each mode of vibration has a fixed number of nodes about which a body will vibrate. A node is a point on the body that does not move relative to the frequency in question[25]. For example in Figure 2.2 (a), a piece of string fixed at both ends is vibrating at the fundamental mode which has no nodes. In the Figure 2.2 (b), the string is vibrating at mode 2, which has one node located at the center.



(a) First or fundamental mode of vibration. (b) First overtone or harmonic.

Figure 2.2. String displaying two different modes of vibration.

An excited body is likely to vibrate with a number of modes. The method of excitation, including location and frequency content, will determine which modes are excited. For example, if a taut string is plucked at the center and then released, mode 2 will not be excited as this has a node at this position[25]. In experiments conducted in [9] where membrane vibrations are studied, the location of excitation is shown to have an impact on the different modes that are excited.

In order to observe the effects of multiple modes of vibration on LVS signature estimation, the target has to be excited to vibrate in multiple modes. The fundamental modes of a body can be stimulated by exciting the body with a tailored appropriate signal, such as a random signal. There are a number of methods to excite a target such as using shakers, impulse hammers and piezoelectric materials. When exciting the body with a random signal, the magnitudes of resonant frequencies will

rise sharply above all other excitation frequencies [13:365-369]. Further examples of different vibrational modes for circular membranes fixed at the rim can be found in Appendix A.

2.5 Modal Analysis

Modal analysis is a method of determining the natural modes of vibration of a structure. There are a number of analytical and experimental techniques that can be employed to determine mode shapes. Finite element analysis, for example, is a popular analytical technique and numerous examples of its use can be found in texts such as [19]. Most of the analytical methods found in texts are complex and require a significant amount of understanding of vibrational physics before they can be employed. Experimentally, Scanning Laser Doppler Vibrometry is a well-established and efficient means of analyzing vibrational behavior of a structure [8].

2.6 Target Selection Considerations

2.6.1 Temperature Fluctuations. Experimental trials in the laboratory showed that some of the targets under consideration were susceptible to temperature fluctuation. When a heat gun was used to flow hot air over a clamped-edge brass target with a radius of 5.08 *cm* and a thickness of 0.0127 *cm*, the resonant frequencies were observed to shift by up to 15 Hz. Thicker targets were tested and found to be more resistant to frequency shift due to temperature. It can therefore be concluded that, thicker targets, which are more thermally stable, are less susceptible to temperature fluctuations and are more likely to maintain stable resonances whilst under investigation.

2.6.2 Complexity of Modal Structure. As shown in Appendix A, round targets have complicated mode structures. A description of the positions of nodes and anti-nodes requires a two dimensional co-ordinate axes. However, on a clamped-clamped beam mounted vertically, only a one dimensional co-ordinate axis is needed

to describe and locate numerous vertical modes. Therefore, to simplify the experiments, a clamped-clamped beam as opposed to a round target is used.

2.6.3 Clamped-Free versus Clamped-Clamped Beam. It is assumed that a clamped-free beam will allow for larger displacements from the relaxed position of the beam than would a clamped-clamped beam. This has potential to bias the results recorded with the LVS as explained below.

Consider a point on a bar ‘X’. As Figure 2.3 (a) shows, point ‘X’ can be displaced horizontally due to vibrational motion of the beam. There are certain points along the journey of ‘X’ at which the laser beam does not “see” the point ‘X’. If ‘X’ happens to be a point of interest (*e.g.* a node of a different frequency) and with the high sampling frequencies sometimes used by the LVS, the node could easily be missed (*e.g.*, if a sample is taken when the mode shape is in the the horizontal position).

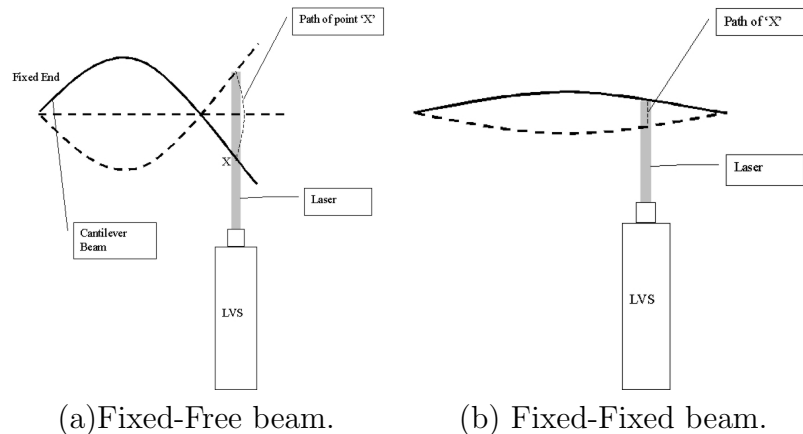


Figure 2.3. Horizontal displacement of points on a clamped-free beam are larger than on a clamped-clamped beam. This can lead to errors. For example in (a), if a sample is taken when the clamped-free beam is in the horizontal position then the point ‘X’ may not be seen by the laser.

2.6.4 Surface Treatment. When the beam is expanded, the signal-to-noise ratio falls due to the resulting drop in intensity. Experiments have shown that the

use of different coatings on targets can result in “substantial reductions” of laser noise due to the relative magnitude of back reflected light to the LVS [30].

2.7 *Signal and Waveform Analysis*

The construction and characterization of power spectral densities (PSD) of vibrational signatures is fundamental to this thesis. A PSD is based on the Fourier transform of a measured time signal such as a voltage signal that contains frequency components, and it indicates how much power there is in each of the frequency components across the observed frequency domain of the given signal. There are many text books that provide insight into the construction of PSD's including [21], [27] and [16]. The method of construction of PSD's can have an effect on the ability of the PSD to effectively estimate the spectral content of a signal. For example, [21:147] indicates how preprocessing the signal with a window can be used to improve the resultant spectral line shape when the PSD is calculated. Increasing the length of the signal (which is not always possible) also improves the spectral line shape making it easier to identify frequency content of the signal. These considerations are taken into account when constructing the PSD's shown in Chapter IV.

2.8 *Laser Beam Propagation*

As indicated in Chapter I, it is necessary to investigate LVS's that are operating at large distances with respect to the target. The diffraction-limited spot size of a laser propagating in the direction, z , can be asymptotically described by [32:70]:

$$w(z \gg z_0) = \frac{\lambda_0 z}{\pi n w_0} \quad (2.2)$$

where

- $w(z)$ = spot size of laser beam
- λ_0 = wavelength of laser used
- z = propagation distance from source
- n = index of refraction of transmission medium
- w_0 = beam waist
- z_0 = Rayleigh range

From Equation 2.2, it is seen that the further away the target is from the laser source, the larger the spot size.

Drain's theoretical discussion of laser interferometry for surface vibration measurement [6] states that, in order to obtain the best Doppler signals, the illuminating measuring spot must be as small as possible so that coherence is maintained over a larger detector aperture. Bearing this in mind, it can be concluded that the optimum signal-to-noise ratio is achieved when the laser is focused on the target. However, in order to simulate a laser beam that has travelled a long distance in the laboratory, the spot size of the laser must be increased. In order to maintain coherence with an increased spot size, a beam expander such as is shown in Figure 2.4 can be utilized.

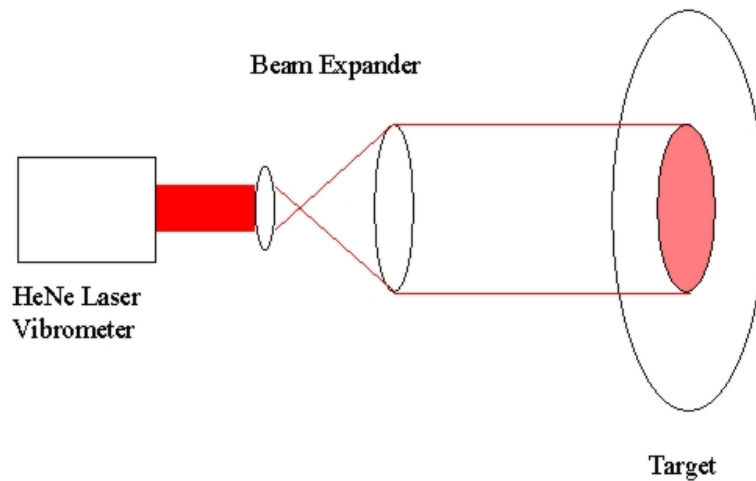


Figure 2.4. Beam Expander - An expanded beam with collimation maintained.

A collimation tester such as the one displayed in Figure B.3 can be used to ensure that the beam exiting the beam expander is collimated.

III. Experiment

3.1 Introduction

In order to investigate the first research goal as described in Section 1.2, some experiments are conducted. This section describes the aim of these experiments. A description of the equipment and settings used, as well as a theoretical and practical modal analysis of the target is, presented. The method used to conduct both a practical experiment and an experiment using a MATLAB® model is described.

3.2 Aim

The aim of these experiments is to determine if spectral line elimination can occur due to a laser spot illuminating a surface that contains multiple velocities when using a Laser Vibrations Sensor (LVS) to perform spectrum estimation.

3.2.1 Multi-Mode Vibration. A body undergoing multi-mode vibration provides a surface which has multiple velocities. If this body is illuminated by a laser that has travelled a long distance and the spot size has increased, the illuminated area of the target may contain components that have velocities of equal and opposite magnitude.

3.2.2 Frequency Spectrum Estimation. As indicated in Section 2.3, the LVS outputs a voltage that is proportional to the velocity being observed by the laser beam. As this is assumed to be a linear system, if the surface contains velocities of equal and opposite magnitude, they should theoretically cancel each other out giving rise to missing spectra in the measured vibrational spectrum.

3.3 Equipment Setup Description and Settings

The general setup for the experiment can be seen in Figure 3.1. The target is a clamped-clamped beam as can be seen in Figure B.1. The LVS is positioned so

that it points through a beam expander to the target. The LVS and beam expander sit atop a plate, whose elevation and azimuth is controlled by a laptop. A signal generator is used to provide the target with an excitation through the use of an amplifier and a piezoelectric transducer. A list and description of the equipment used to conduct the experiment is contained in Appendix B. More detail about the equipment settings is outlined below.

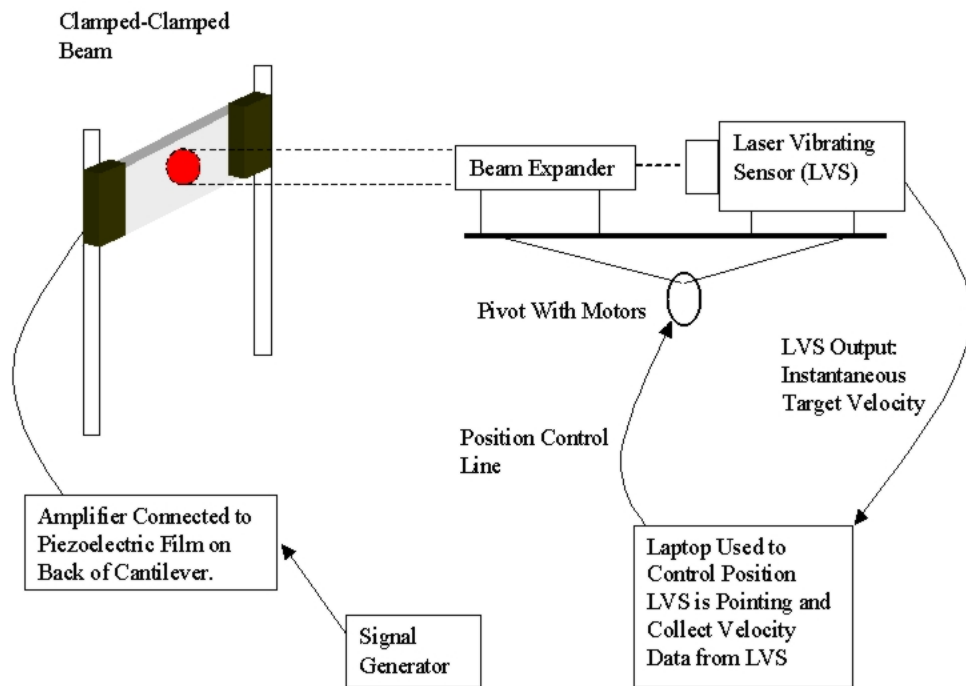


Figure 3.1. General set-up of experiment.

3.3.1 Laptop Settings. The main use of the laptop is to control the position of the directed laser energy, as well as to sample and record the output from the LVS, which is a voltage representative of the instantaneous velocity of the target. The recorded file format is shown in Appendix C. The sampling settings listed in Table 3.1 was used. A sampling rate of 20 KHz is high, and it allows samples to be taken reasonably quickly. This is advantageous when many samples are to be taken. A sampling length of 4096 samples was found to be adequate to obtain accurate

frequency information. Averaging ten recordings per point gives aesthetic results for plots that are to be analyzed.

Table 3.1. Sampling Settings.

Sampling Rate	20Khz
Number of Samples per Point	4096
Number of Recordings per Point for Averaging	10

3.3.2 LVS Settings. The LVS settings are listed in Table 3.2 for the sake of repeatability of the experiments to be conducted.

Table 3.2. LVS Settings.

Output Velocity Range	5mm/S/V
Frequency Filter	5KHz
Tracking Filter	Slow

3.3.3 Laser Beam. In order to obtain a reading with maximum signal-to-noise ratio, the laser beam should be focused on the target [23]. While performing modal analysis as outlined in Section 3.4.3, the laser beam is focused on the target. However, in order to simulate a laser beam that has travelled a large distance and has an enlarged spot size, the beam expander is employed in line with discussion in Section 2.8. The beam is expanded, and a collimation tester is used to confirm that the beam is collimated.

3.3.4 Signal Generator and Amplifier. The signal generator is set up to output a 1-volt random signal, with frequencies ranging from 1 Hz to 5 KHz. The amplifier is set to use 20X amplification. The output that is sent to the piezoelectric film is thus a 20-volt 1Hz-5KHz random signal.

3.4 Clamped-Clamped Beam as a Target

A clamped-clamped beam is selected as a target to conduct the experiment. Such a target provides easily locatable nodes and anti-nodes when undergoing ran-

dom excitation. These nodes are vertical with respect to the horizontally placed beam, allowing for easier location as discussed in Section 2.6.2.

3.4.1 Target Surface. Experimental results in the lab have shown that highly reflective diffuse surface treatment leads to a stronger signal-to-noise ratio. When the laser beam is in expanded beam mode, the signal-to-noise ratio proved to be too small to collect meaningful results from an uncoated target. This problem was overcome by coating the surface with a highly reflective diffuse sticker.

3.4.2 Theoretical Modal Analysis of Eigenfrequencies of Target. The eigenfrequencies of the beam are calculated using Euler-Bernoulli beam modelling as outlined in [13]. This provides information on where to focus attention when using the LVS to examine the target, as well as verification that the LVS is being used correctly.

The beam is known to have the physical properties outlined in Table 3.3.

Table 3.3. Physical properties of beam.

Young's Modulus, E	62052815638.5 Pa
Moment of Inertia I	$1.8606 \times 10^{-11} m^4$
Length l	0.278 m
Mass per unit length μ	.1862 kg - m ⁻¹

The natural frequencies of the beam can be calculated using the following equation [13].

$$\omega_n = \frac{(\lambda_n l)^2}{2\pi} \sqrt{\frac{EI}{\mu l^4}} \quad (3.1)$$

where

- ω_n = n^{th} natural frequency
 $\lambda_n l$ = weighted frequency
 E = Young's Modulus
 I = Moment of inertia
 l = length of clamped section of beam

The first six values of $\lambda_n l$ can be found in table 3.4 and are taken from [13:335]. Using equation 3.1, the first six eigenfrequencies are then calculated and the results are displayed in Table 3.5.

The mode shape of a clamped-clamped beam can be described by the following equation [13:335]:

$$\cosh(\lambda_n x) - \cos(\lambda_n x) - \sigma_n (\sinh(\lambda_n x) - \sin(\lambda_n x)) \quad (3.2)$$

where

$$\sigma_n = \frac{\cosh(\lambda_n l) - \cos(\lambda_n l)}{\sinh(\lambda_n l) - \sin(\lambda_n l)}$$

The first six mode-shapes are plotted in Figure 3.2.

Table 3.4. First six values of $\lambda_n l$.

$\lambda_1 l$	4.73004074
$\lambda_2 l$	7.85320462
$\lambda_3 l$	10.9956079
$\lambda_4 l$	14.1371655
$\lambda_5 l$	17.2787597
$\lambda_6 l$	20.4203522

3.4.3 Practical Modal Analysis of Eigenfrequencies of Target. It is required that locations of nodes and anti-nodes of the different modes on the clamped-clamped beam are known. Practically, this requires a modal analysis in order to characterize

Table 3.5. Calculated eigenfrequencies ω_n of beam.

ω_1	112Hz
ω_2	308Hz
ω_3	605Hz
ω_4	1001Hz
ω_5	1495Hz
ω_6	2088Hz

the clamped-clamped beam. The method selected to perform the modal analysis is to use the focused LVS.

The clamped-clamped beam is excited with a random signal that contains frequencies from 1Hz - 5KHz. A grid of points is then created using the computer that controls the laser. The laser is focused onto the target and directed to move to each of the grid points and record the surface velocities. Photographs of the laser whilst at each point on the target were taken. These photos were averaged together to obtain Figure 3.3.

The velocities and positional information is then imported into MATLAB®. The program in Appendix D is used to calculate the average PSD (of ten recorded waveforms) at each of the points at which the laser was directed on the target. A Hanning window is then used to pre-process the data. It has the effect of smoothing the data at each end of the record, and thus sharpening the spectral window when the Fourier transform is taken. The PSD between the measured data points is then interpolated. Frequency bins are generated and, at each frequency bin, the spatial frequencies are plotted. The different spatial modes can then be observed by individually viewing the different frequency bins. This is easily converted to an *avi* file that can play a “movie” displaying the different frequency bins. The advantage of having a movie is that it allows quick eigenfrequency identification by playing the movie and watching for changes. A sample observation of a frequency bin located at 1469 Hz can be seen in Figure 3.4.

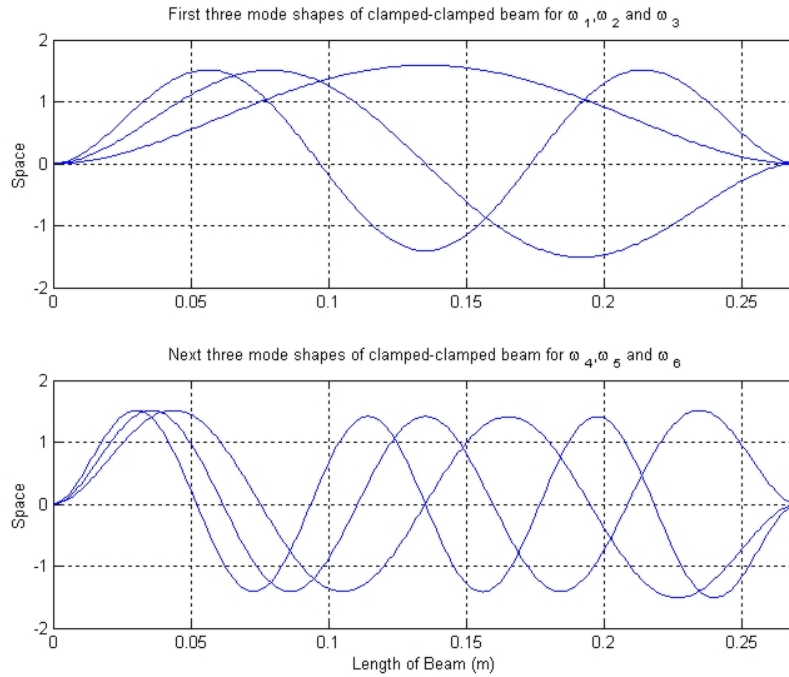


Figure 3.2. Plots of the first six modes shapes with the amplitude arbitrarily normalized for display purposes.

Spatial frequencies identified using this technique are displayed in Figure 3.5. These locations can easily be scaled onto the beam to locate the spatial nodes as shown in Figure 3.6. These frequencies are shown to match up well to the calculated eigenfrequencies in Table 3.5. The slight discrepancies can be attributed to:

1. The clamped-clamped beam has a reflective sticker which would affect its vibrational properties.
2. On one end of the clamped-clamped beam, the clamp is slightly lipped. That is the clamp on the back side does not match up vertically to the clamp on the front side by approximately 3 cm.

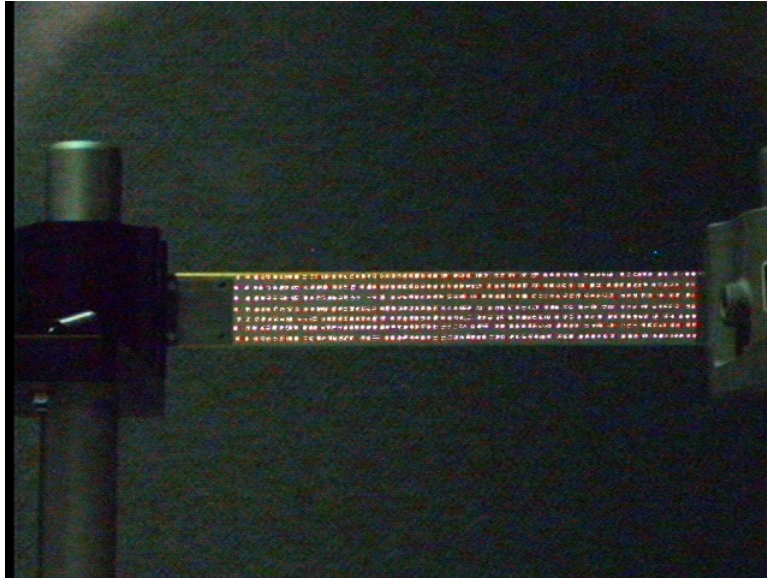


Figure 3.3. Beam showing points where LVS measured the surface velocities.

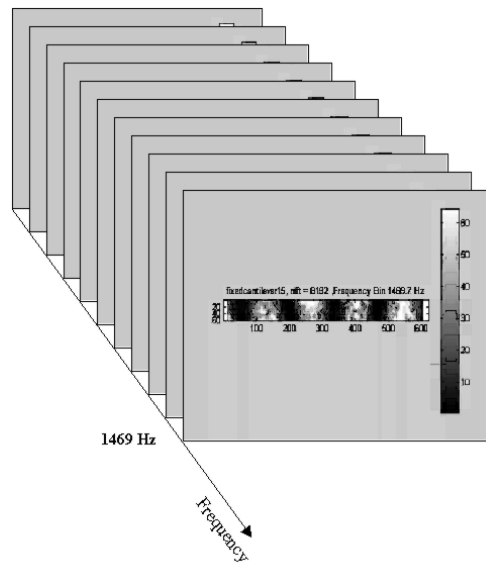


Figure 3.4. Spatial frequencies on clamped-clamped beam observed at 1469 Hz. The darker shaded areas are indicative of nodal points and are not moving with respect to the 1469 Hz signal.

3.5 Modeling Experiment

A model of the clamped-clamped beam was created using MATLAB®. The code is listed in Appendix E. The first six mode shapes as calculated in Section

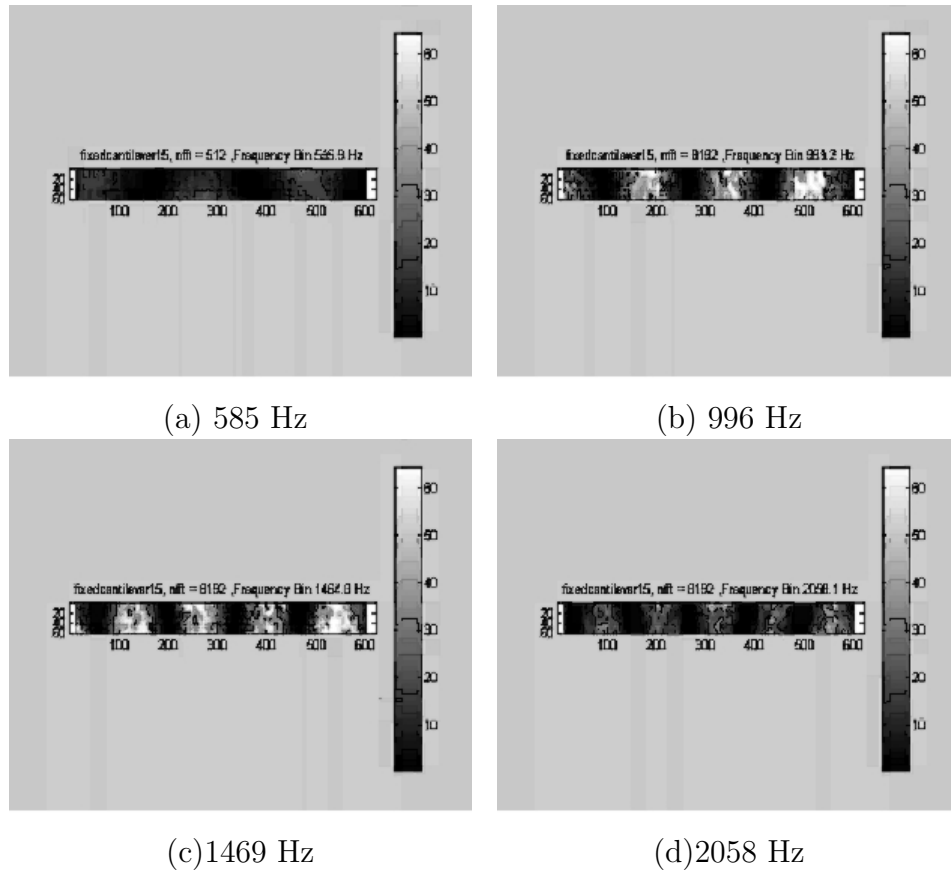


Figure 3.5. Some of the spatial frequencies identified on the randomly excited clamped-clamped beam.

3.4.2 are programmed to vibrate with their respective eigenfrequencies on the beam. A simulated (LVS) is then used to illuminate the clamped-clamped beam. The illuminating laser spot can be moved horizontally along the beam. The width of the beam can also be varied to simulate distance from the laser source. The simulated LVS will then calculate an output voltage proportional to the velocity of the illuminated area on the beam. This model can be used to predict how the LVS will behave when illuminating multiple velocities on a target.

3.5.1 Assumptions and Simplifications. To simplify the model, a number of assumptions are made about an LVS system and target.

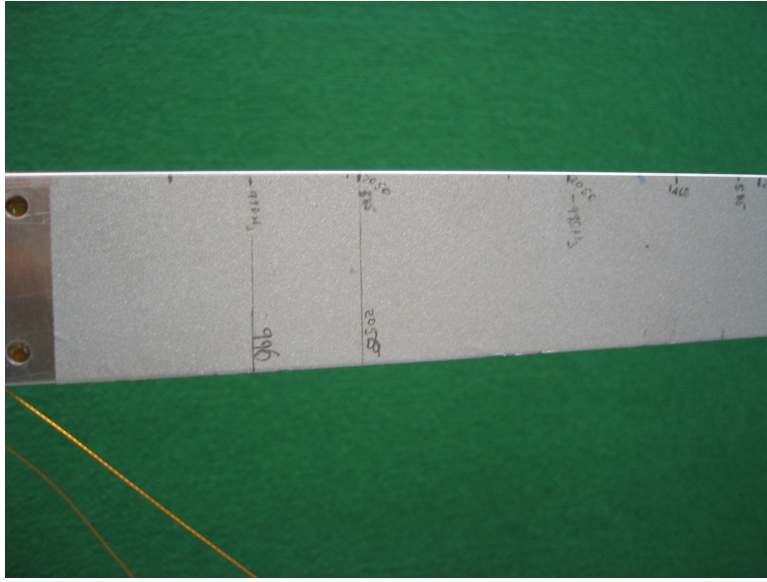


Figure 3.6. Section of clamped-clamped beam showing points where vertical nodes at 996 Hz and 2058 Hz have been identified.

3.5.1.1 Laser Modes. Laser beams have Gaussian intensity profiles as is shown in [32] and can lase in a number of modes. The model simulates a laser-beam with a Gaussian profile in the first mode. The LVS used in the experiments is designed so that the laser contains no more than two modes as indicated in [23].

3.5.1.2 Projection of Illuminated Area. It is also assumed that the amplitude of the clamped-clamped beam vibrations are small enough that they do not effect the amount of signal returning to the laser.

3.5.1.3 Modeling of Target Surface. For the practical experiment, the target is a highly reflective diffuse coating as described in Section 3.4.1. However, in the model, the surface is modeled as a specular surface. This will allow observation of signal washout effects in relation to the position of the laser and the shape of the vibrational mode.

3.6 Experimental Procedures

There are two experiments that are conducted to confirm if higher order modes of vibration are capable of eliminating spectral content. The first one is a practical experiment, and the second is an experiment performed with the model created using MATLAB®.

3.6.1 Practical Observation of Multi-Modal Effects. Once the locations of nodes and anti-nodes have been identified on the target, the laser is then expanded to simulate the effect of having travelled a long distance and diverged, resulting in an enlarged diameter. The beam expander is set up to ensure that the output beam that hits the target is collimated. The expanded laser beam is then used to illuminate different areas of the characterized target, and results are collected for analysis.

Observations are made on different areas of the target to determine if there are different effects on the frequency spectrum due to the location of the laser with respect to the different nodes and anti-nodes present. These observations include observing the following nodes derived from the practical nodal analysis:

1. Expanded beam over node at 2058 Hz.
2. Expanded beam over nodes at 1469 Hz and 996 Hz.
3. Expanded beam over node at 585 Hz.

3.6.2 Use of Model to Observe Multi-Modal Effects. The model is then used to generate the true PSD of the simulated clamped-clamped beam. This is achieved by focusing the simulated laser beam onto a section of target that is known to have no nodes. This point is found to be 0.11 m in the x-direction (0.11 m from the left clamped edge). Once the true PSD is known, the simulated laser beam is used to illuminate nodes that were programmed into the simulated target. These nodes belonged to the calculated frequencies of Table 3.5, and the laser is placed over these nodes so that there is an equal amount of laser beam illuminating both

sides of the node. Observations are then made. The laser beam is then moved in small increments away from the node to see if there is any relationship between the PSD and the position of the laser away from the node.

IV. Results and Analysis

4.1 Introduction

In this chapter, results for both the practical experiment, and the simulated experiment are presented and analyzed.

4.2 Experimental Results

Results of the experiments are outlined below.

4.2.1 Expanded Beam Over Node at 2058 Hz. Figure 4.1 shows the PSD of an expanded laser beam from the LVS illuminating a node at 2058 Hz. The expanded laser beam is directed so that the node of that frequency runs vertically down the clamped-clamped beam through the center of the illuminated area. This results in the area of the target containing two areas of equal and opposite phase with respect to the 2058 Hz frequency that exists on the clamped-clamped beam. The PSD shows that the spectral line at 2058 Hz is almost non-existent. When half of the laser beam is blocked from reaching the target, the return signal only contains spectral information associated with the left side of the node. This information is no longer washed out (eliminated due to photons carrying equal magnitude and opposite phase information) and the spectral line at 2058 Hz is seen to be strong, with an increase of 20 dB/Hz. This can be seen in Figure 4.2.

The experiment is repeated for a number of different frequencies, and the results are outlined below.

4.2.2 Expanded Beam Over Nodes at 1460 Hz and 996 Hz. The experiment is repeated at nodes of 1460 Hz and 996 Hz. The same observations are seen as with the node at 2058 Hz. In Figure 4.3, the expanded beam is centered around a node at 1460 Hz, and the PSD shows that this frequency has a small peak of approximately

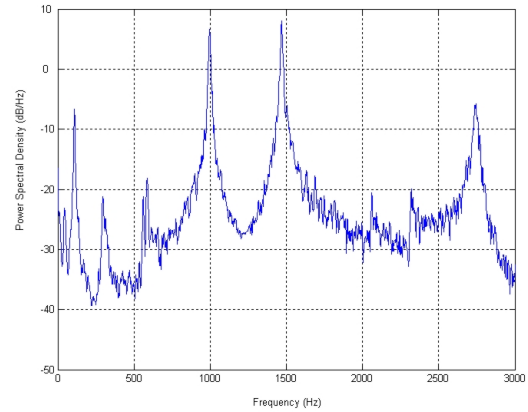
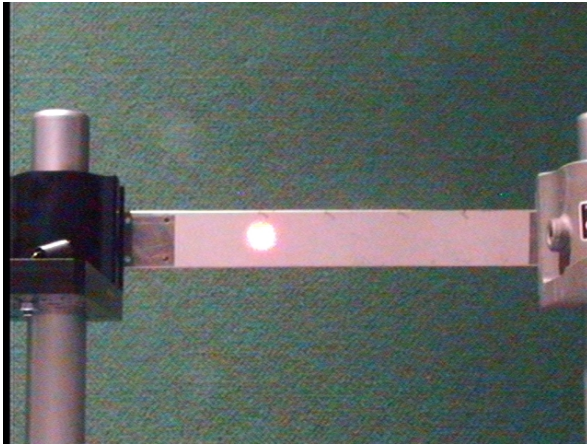


Figure 4.1. Expanded beam illuminating node at 2058 Hz and associated PSD. Notice the near annihilation in the 2058 Hz spectral line power.

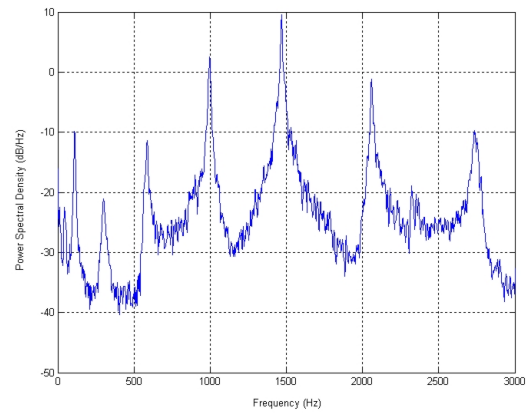
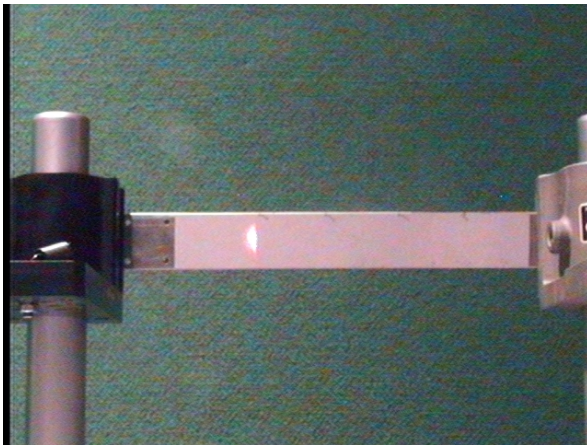


Figure 4.2. Expanded beam partially blocked illuminating only one side of node at 2058 Hz and associated PSD. Notice the strong return of the spectral line at 2058 Hz.

-20 dB/Hz. In Figure 4.4, when the beam is blocked from illuminating one side of the node, the spectral line increases in power by about 20 dB/Hz. The spectral line missing at 2700 Hz in Figure 4.4 is due to the remaining illuminated area of the beam positioned on the node at 2700 Hz.

In Figure 4.5, the spectral line at 996 Hz is not obvious. However, when half the illuminated area is blocked, then the spectral line emerges and rises 20 dB/Hz, as shown in Figure 4.6. Again the spectral line missing at 2700 Hz in Figure 4.6 is

due to the remaining illuminated area of the beam sitting on a node of the 2700 Hz mode.

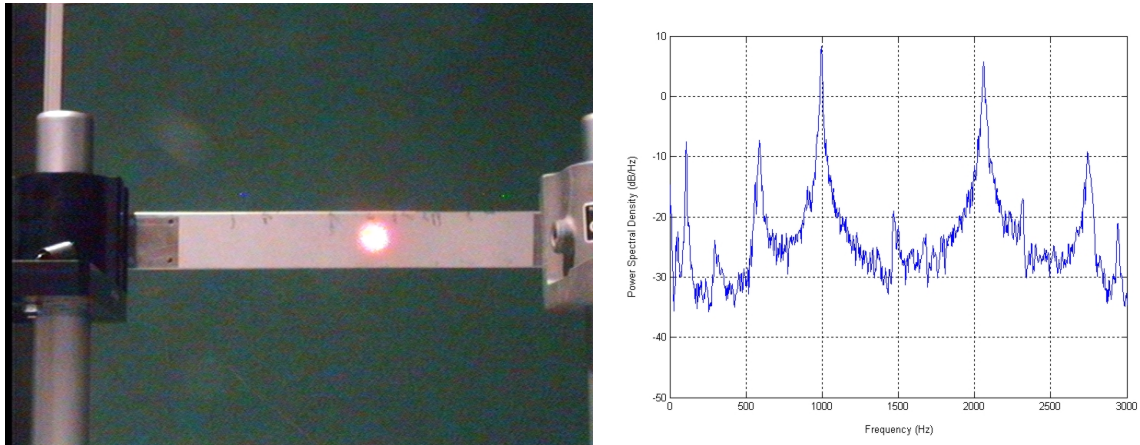


Figure 4.3. Expanded beam illuminating node at 1460 Hz and associated PSD. Notice the peak at 1460 Hz has a small magnitude in comparison to the other eigenfrequencies of the beam.

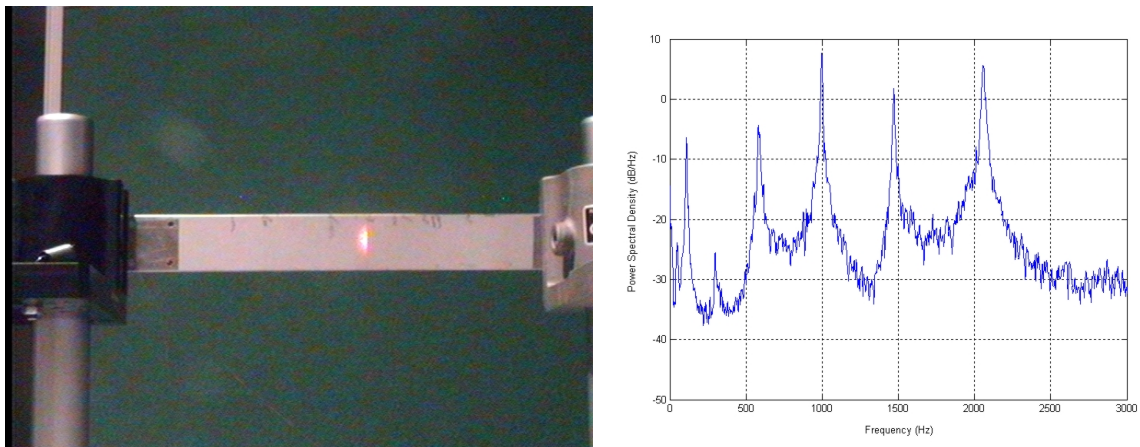


Figure 4.4. Expanded beam partially blocked illuminating one side of node at 1460 Hz and associated PSD. Notice the strong return of power in the signal at 1460 Hz. This is a nodal point for the 2700 Hz signal which explains why it is missing from the PSD.

4.2.3 *Expanded Beam Over Node at 585 Hz.* Attempts to examine spectral elimination at 585 Hz resulted in an observed signal reduction of approximately 6 dB/Hz. This can be seen in Figures 4.1 and 4.2 which also happens to be a node for

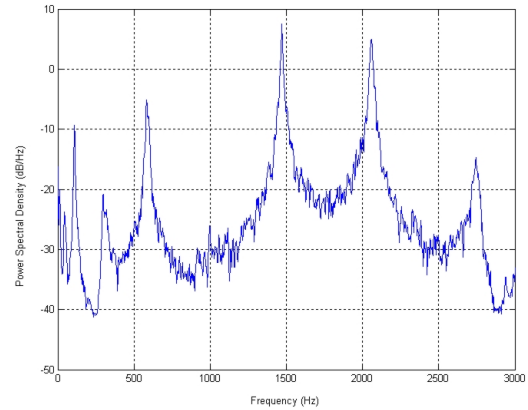
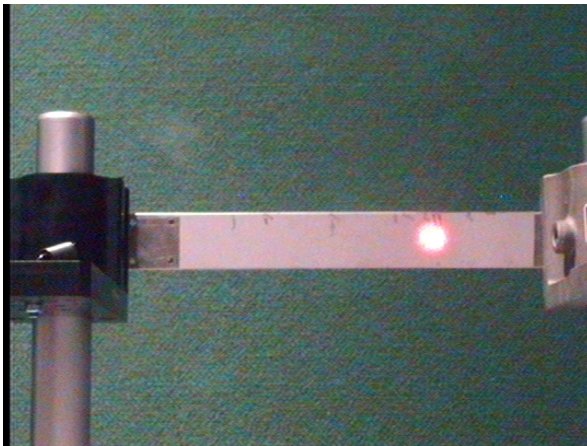


Figure 4.5. Expanded beam illuminating node at 996 Hz and associated PSD. Again the spectral line at 996 Hz is almost non-existent

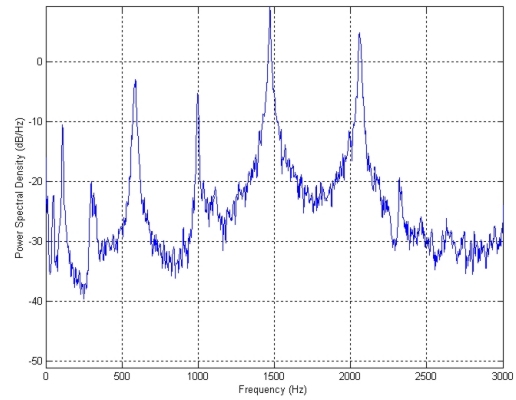
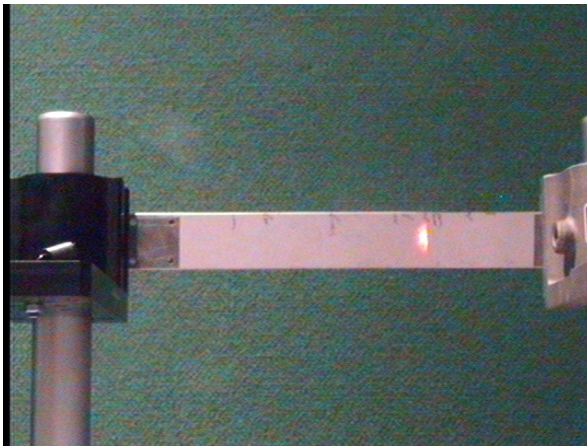


Figure 4.6. Expanded beam partially blocked illuminating one side of node at 996 Hz and associated PSD. Notice the rise in power of the spectral line at 996 Hz.

the 2058 Hz frequency. It is assumed that the lower frequencies are less stable in the clamped-clamped beam causing nodes to shift slightly, thus reducing the strength of effective spectral elimination.

4.3 Simulation with MATLAB® model Experiment Results

The results using the simulator are shown in the Figures 4.7 - 4.12 below. Figure 4.7 shows the true vibrational spectrum of the clamped-clamped beam. In

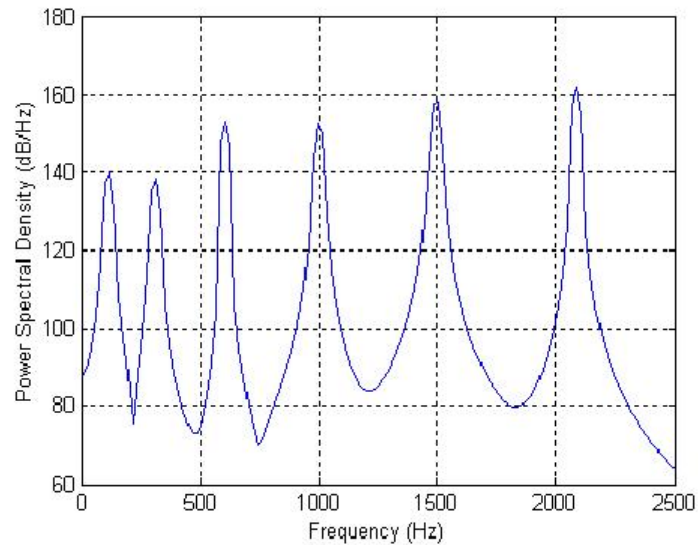


Figure 4.7. True PSD of clamped-clamped beam showing all six eigenfrequencies programmed into the beam.

Figure 4.8, when the simulated laser beam is used to illuminate a node that is common to mode 2 (308 Hz), mode 4 (1001 Hz) and mode 6 (2088 Hz) of the clamped-clamped beam, all three of the frequencies are washed out. Again in Figure 4.9 and Figure 4.10, the frequencies at 605 Hz and 1495 Hz are seen to be annihilated when the LVS is centered around their respective nodes.

4.4 Peak PSD as LVS is Moved Away from Node

As the LVS is moved away from the washout condition, the spectral lines at the missing frequencies rise as can be seen in Figure 4.11. This shows that there is immediate response as soon as the laser moves off of the washout condition. The plots of these spectral peaks are plotted in Figure 4.12 to examine if there is any relationship between the mode shape of the target, the frequency that it is vibrating at, and the amount of movement away from the node in relation to the amount of signal return. As can be seen from Figure 4.12, it is found that in the first 0.009 m there is no significant difference between the rate of signal return and the amount of distance that the laser is moved away from the node.

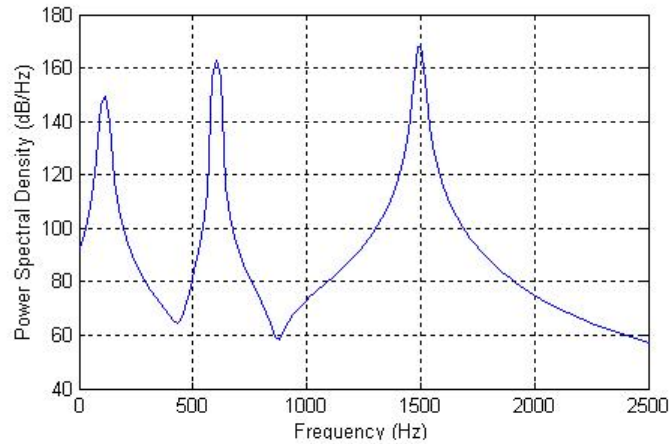


Figure 4.8. PSD of Simulated LVS illuminating node common to mode 2 (308 Hz), mode 4 (1001 Hz) and Mode 6 (2088 Hz). Notice all three frequencies are missing from the PSD.

4.5 Experimental Conclusions

These results show that spectral lines are susceptible to elimination due to multi-mode vibrational effects. When the illuminated area of a target contains two equal areas that have velocities that are in equal and opposite phase of vibration, then signal washout of the associated vibration frequency is observed. The results are confirmed by the simulated model of the situation.

In the practical experiment, the spectral elimination observed was based on ten readings at a nodal point. Once a stable nodal position was found and spectral elimination was observed, then a slight movement of the target would result in an increase of power in the spectral line. It was found that if more slight movement was made in the same direction, then another point where spectral elimination could be observed would occur. This suggests that the surface properties (reflectivity and optical roughness) play a part in the returned positional intensity, and are therefore important in determining whether the number of photons carrying velocity information of equal and opposite phase will cancel each other out.

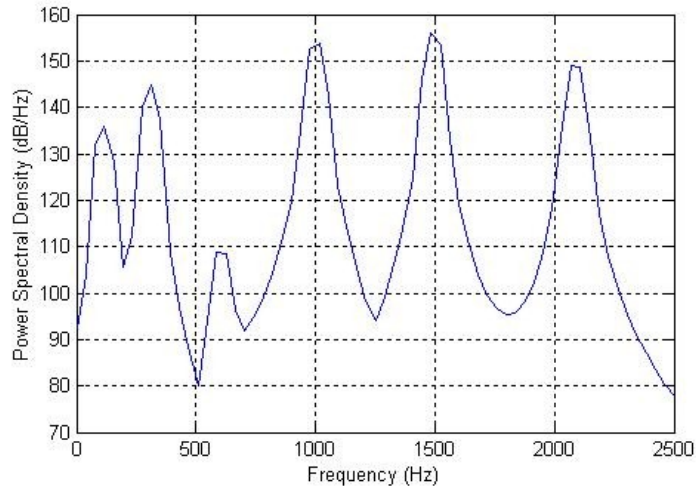


Figure 4.9. PSD of Simulated LVS laser spot centered around node at 605 Hz.

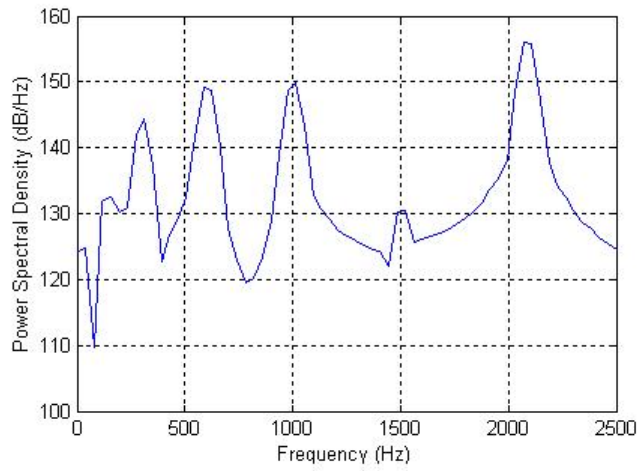


Figure 4.10. PSD of Simulated LVS laser spot centered around node at 1495 Hz.

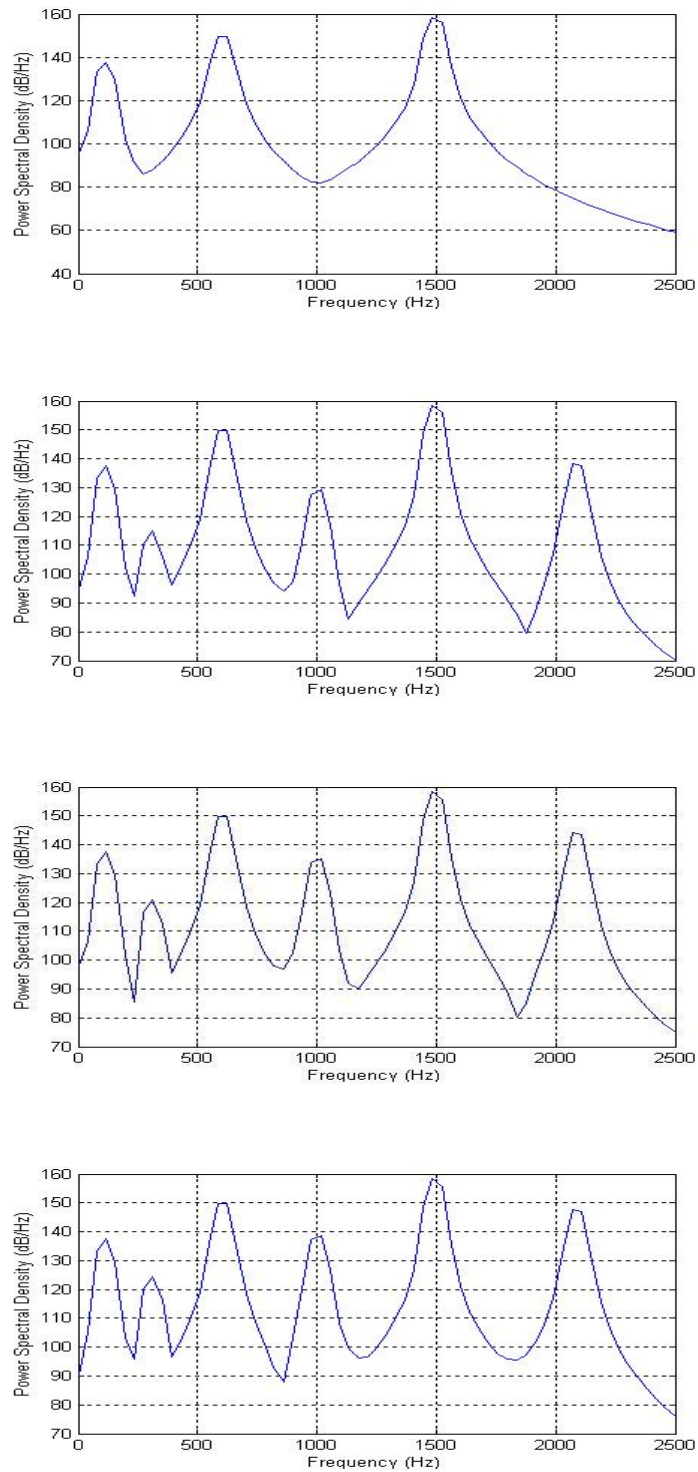


Figure 4.11. PSD of target as laser is moved in 0.001 m increments away from washout condition at the node common to frequencies 605 Hz, 1001 Hz and 2088 Hz. This Figure shows the first four incremental moves.

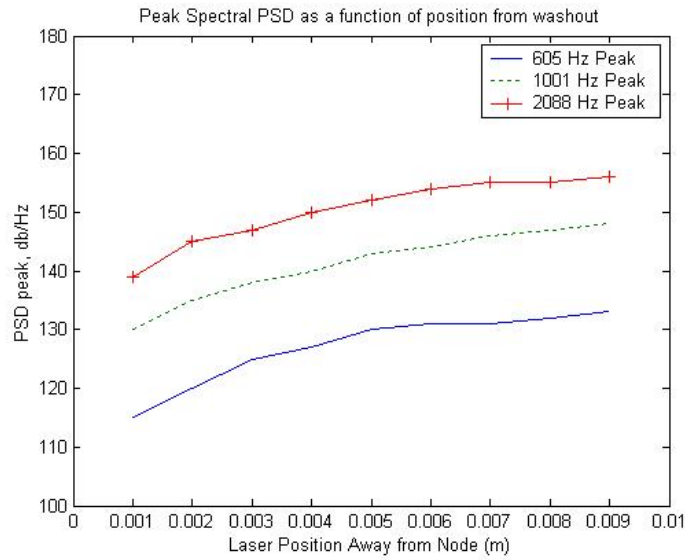


Figure 4.12. Peak spectral PSD for spectral lines at 608 Hz, 1001 Hz and 2088 Hz as the simulated LVS is moved away in 0.001 increments away from washout condition. This Figure shows the first nine incremental movements. This result is specific to the set-up used to conduct this experiment.

The MATLAB® model also shows that a very small movement away from the washout condition results in the spectral lines returning.

V. Mitigating Spectral Elimination

5.1 Introduction

In this chapter, preliminary efforts are made to examine methods to mitigate the effects of spectral peak elimination during spectrum estimation via LVS. Methods investigated are continuous scanning of target, laser blocking and signal processing techniques. These methods are expanded on below.

5.2 Target Measurement using Continuous Scanning Techniques

“Laser Doppler Vibrometer has the particular capability of being able to measure the vibration of an object whilst the measurement point is being scanned over the surface [29]”. It is therefore sensible to investigate if continuous scanning techniques are more resistant to the spectral elimination effects observed in Chapter IV.

5.2.1 Theory. For the experiments described in Chapter III, all measurements of the velocity were taken with the target and LVS stationary with respect to each other. If measurements were made while the laser beam was scanning the target, then spectral elimination should theoretically be reduced, if not eliminated. This is due to the fact that the points in time at which the spectral elimination occur would only be observed for a fraction of the time of the scan - depending on the scanning velocity and number of nodes crossed.

5.2.2 Experimental Scanning Laser Across Nodes. An experiment was conducted to test if scanning techniques could possibly give rise to reduction in signal washout effects. The LVS hardware-software control does not allow for collecting data while scanning. However, the target position can manually be adjusted horizontally. Adjusting the target horizontally while the laser is collecting data will

therefore produce the same results as a laser that had the ability to scan the target and simultaneously collect data.

For the previous experiments in Section III, the sampling rate was set at 20 KHz. For 4096 samples (which is the number of samples being taken per reading), this would require a time of 0.205 seconds ($1/20000 * 4096$) to acquire one record. Therefore, in order to take advantage of the laser scanning a node, the target would have to be adjusted within the 0.205 second sampling period. The only mechanics available to adjust the target were by human operator (very slow reaction time and uneven velocity). Therefore, the lowest frequency that displays significant signal washout (996 Hz) is selected to observe the effects of scanning a node. While trying to observe a 996 Hz signal, the sampling frequency can be dropped to a Nyquist rate of 1980 Hz. However, 2100 Hz is selected as this will allow for better presentation of results. At 2100 Hz, the sample time is 1.95 seconds ($1/2100 * 4096$) which is enough time for a human operator to quickly adjust the target once sampling has commenced. The start and end position of the scan can be seen in Figure 5.1.

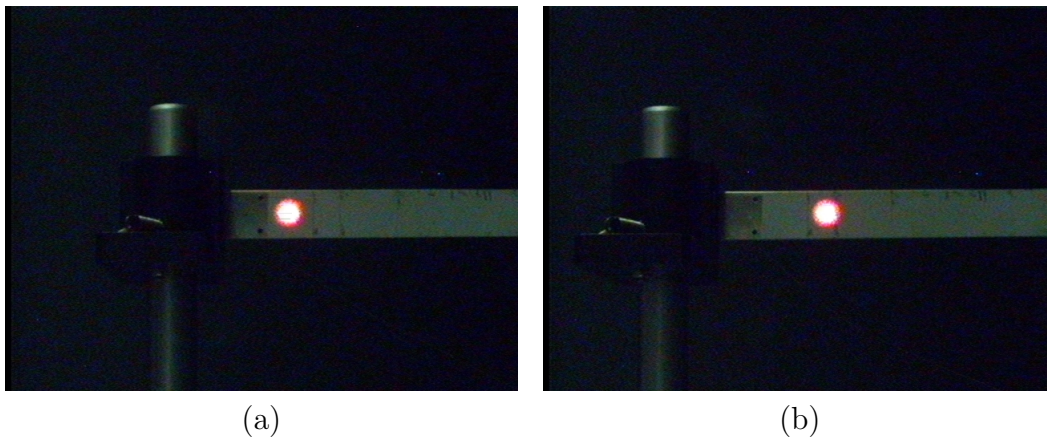


Figure 5.1. Scanning across a 996 Hz node. (a) Position of laser on target at beginning of scan and (b) position of laser on target at end of scan.

5.2.3 Results and Conclusions of Continuous Scanning Techniques. The practical results obtained were not under ideal lab conditions as the target was

adjusted by hand. However, in Figure 5.2, it can be seen that 996 Hz is observed. The scanning velocity is estimated to be approximately $0.05 \text{ m} - \text{s}^{-1}$.

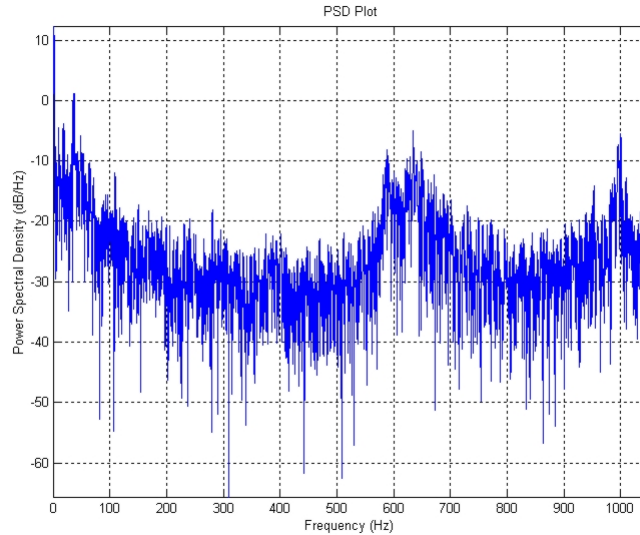


Figure 5.2. PSD showing 996 Hz peak observed while scanning across the node.

Theoretically, a scanning technique could be used. It is known that continuous scanning techniques have been used for modal shape analysis in a number of different circumstances, as can be found in [29], [9], [3], [8], [2] and [4].

5.3 Laser Blocking at Source

5.3.1 Theory. Figure 5.3 shows a circular aperture and its Fourier transform. The Fourier transform of an aperture shows the intensity of the Fraunhofer diffraction pattern of a unit-amplitude plane wave that passes through the aperture [14].

Figure 5.4 shows the same aperture half blocked. What can be noted in this figure is that by half blocking the aperture, there develops a line of intensity (in this case the line is horizontal owing to a vertical block). In Section 4.5, it was noted that the reflectivity and the positional intensity of the laser on the target was

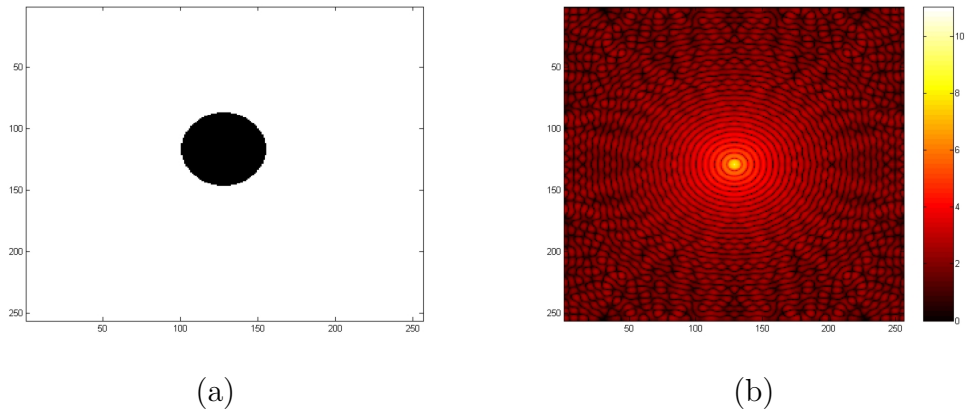


Figure 5.3. (a) Circular aperture and (b) its Fourier transform.

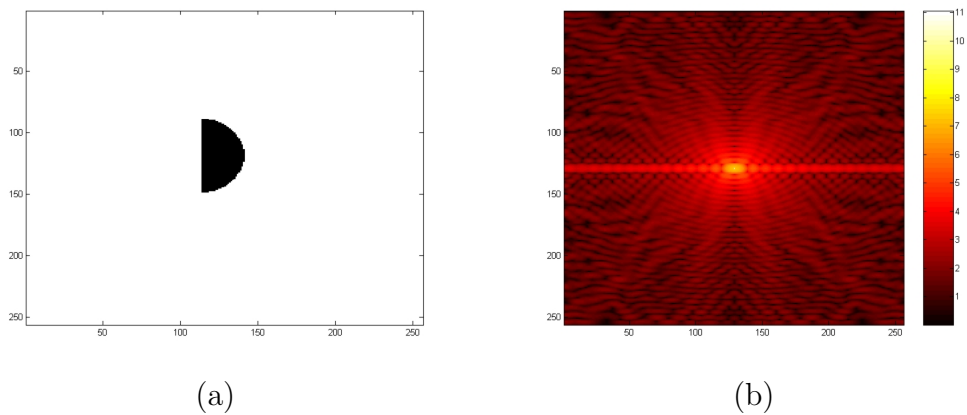


Figure 5.4. (a) Half of a circular aperture and (b) its Fourier transform.

important in determining if spectral elimination occurs. Therefore, changing the intensity pattern could potentially expose the “hidden” frequencies.

5.3.2 Laser Blocking Experiment. A small experiment was conducted by placing the laser over a node at 2096 Hz. The PSD was recorded; then the laser was half blocked at the source and the PSD recorded again. These results are shown in Figure 5.5.

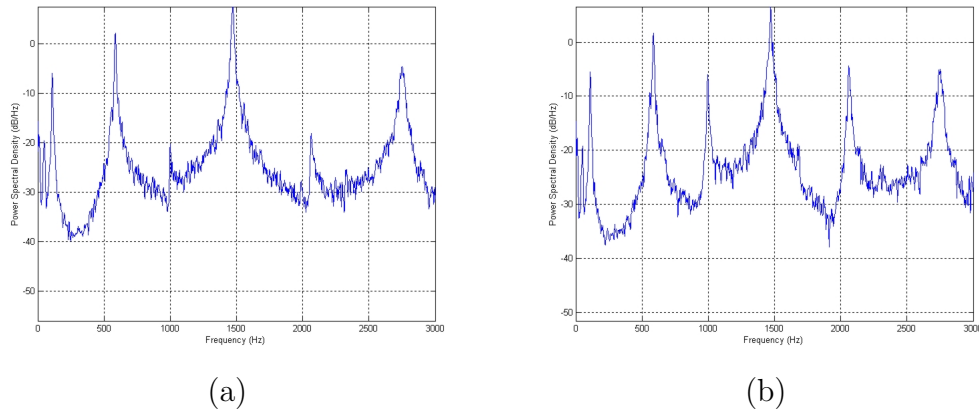


Figure 5.5. PSD showing the rise in spectral line at 2058 Hz and 996 Hz when the intensity pattern is changed by half blocking the laser.

5.3.3 Conclusion. The method of changing the intensity pattern on the target is shown to work experimentally. However, this method does reduce the total intensity at the target, and hence would be more susceptible to noise.

5.4 Signal Processing Techniques Discussion

The results obtained in Section IV indicate that, even during spectral elimination, there is still a small amount of the signal remaining. That being the case, then other signal processing methods to perform enhanced spectrum estimation can be used to identify these spectra. Reference [7] indicates that Bayesian frequency estimators dramatically outperform Fast Fourier Transform (FFT) approaches. These methods take into account what is already known about the signal to be estimated, and have shown superior performance, especially when the measurement time is limited as would be the case in the battle-field. The paper concludes that the Bayesian approach used to estimate a single sinusoid model yields a frequency estimate that is accurate to approximately 1% over a short time series. This is an improvement by nearly two orders of magnitude upon the estimate obtained from FFT.

VI. Conclusions and Recommendations

6.1 Restatement of Research Goal

As stated in Section 1.2, the goals of this research are to:

1. Determine if multi-mode vibrations can eliminate spectral line content from the vibrational spectrum of a target when using an LVS.
2. Perform preliminary investigations into methods of mitigating any negative effects caused by multi-mode vibrations during the spectrum estimation process.

6.2 Conclusion

The results observed are based on a continuous scanning laser. To apply these results to a pulsed laser requires considering only the first few sampled points of the target to be for use in calculating spectra.

6.2.1 Multi-Modal Impact on Signature Estimation. First, it has been shown empirically in Section IV that bodies vibrating in modes higher than the fundamental mode have the ability to eliminate spectral lines while using an LVS to perform spectrum estimation. This is a phenomenon that requires almost precise positioning of the laser about the node. In addition, the reflected intensity pattern due to the diffuse surface pattern plays a role in determining the exact positions around a node at which spectral elimination will occur. The experiment conducted using the MATLAB® model of the situation confirms the results observed in the practical experiments.

6.2.2 Mitigation of Multi-Modal Impacts. Preliminary investigations into mitigating the observed spectral elimination effects show that there are a variety of methods that have potential to be utilized. The methods considered, laser scanning,

laser blocking at source, and signal processing techniques, all show promise in their ability to expose missing spectral lines.

6.3 Recommendations

The practicality of implementing methods to mitigate missing spectral lines should be considered, and then methods determined to be viable should then be investigated further.

*Appendix A. Examples of Modes of Vibration of a circular
Membrane taken from [25]*

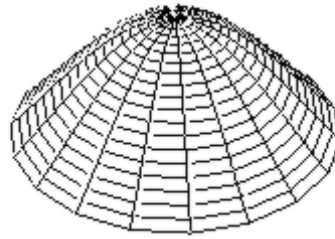


Figure A.1. The (0,1) Mode. The mode number is designated as (0,1) since there are no nodal diameters, but one circular node (the outside edge). A node is a point (or line) on a structure that does not move while the rest of the structure is vibrating. The (0,1) mode of a drum, is excited when the drum head is struck at its center. When vibrating in this mode the membrane acts much like a monopole source, which radiates sound very effectively. Since it radiates sound so well when vibrating in this manner, the membrane quickly transfers its vibrational energy into radiated sound energy and the vibration dies away. The short duration (fraction of a second) of the (0,1) mode means that this mode does not contribute greatly to the musical tone quality of a drum. In fact, when struck at the center a tympani, or other large drum, produces a "thump" which decays quickly and with no definite pitch.

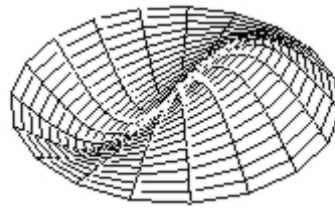


Figure A.2. The next mode is the (1,1) with one nodal diameter and one circular node (the outside edge). The exact location of the nodal diameter depends on the homogeneity of the membrane and the initial conditions when the vibration starts. The frequency of the (1,1) mode is 1.593 times the frequency of the (0,1) mode. When vibrating in the (1,1) mode a circular membrane acts much like a dipole source; instead of pushing air away from the membrane like the (0,1) mode does, in the (1,1) mode one half of the membrane pushes air up while the other half sucks air down resulting in air being pushed back and forth from side to side. As a result, the (1,1) mode radiates sound less effectively than the (0,1) mode which means that it does not transfer its vibrational energy into radiated sound energy as quickly as the (0,1) mode and therefore, the (1,1) mode takes longer to decay. Because the (1,1) mode "rings" for a while, it contributes to the musical sound or pitch of a drum. When a tympani, or other large drum, is struck somewhere between the center and outer edge, the sound has a definite pitch which lingers for a several seconds.

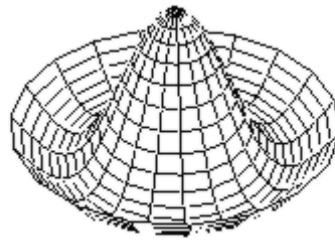


Figure A.3. The (0,2) mode, shown above does not have any diameter nodes, but has two circular nodes - one at the outside edge and one at a distance of $0.436 a$ (a is the radius of the circular membrane) from the outer edge. The frequency of the (0,2) mode is 2.295 times the frequency of the (0,1) mode. Like the (0,1) mode, the (0,2) mode is excited when the membrane is struck at the center. The sound radiation characteristics of the (0,2) mode are more complicated than the first three modes – it appears to be a mix between a monopole and a dipole. Its decay time is longer than the (0,1) mode, but shorter than the (1,1) mode. As a result, it contributes to the "thump" sound when a drum is hit at the center, but does not contribute much to the musical pitch of a drum when

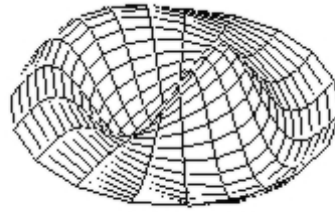


Figure A.4. The (1,2) mode has one nodal diameter and two nodal circles. The frequency of the (1,2) mode is 2.917 times the frequency of the (0,1) mode. As you might expect after looking at the first several modes of the circular membrane, the (1,2) mode does not radiate sound very effectively. It has somewhat of a quadrupole type behavior. Thus, the (1,2) mode takes a relatively long time to decay. However, this mode doesn't seem to play a dominant role in the musical tone quality of a drum.

Appendix B. Equipment List

Clamped-clamped Beam	Figure B.1
Amplifier	Figure B.2
Collimator Checker	Figure B.3
Onisoki FFT Analyzer and Signal Generator	Figure B.4
Polytech Sensor Head OFV-353.	Figure B.5
Laptop For Recording and Position Control	Figure B.6
Beam Expander	
Camera	

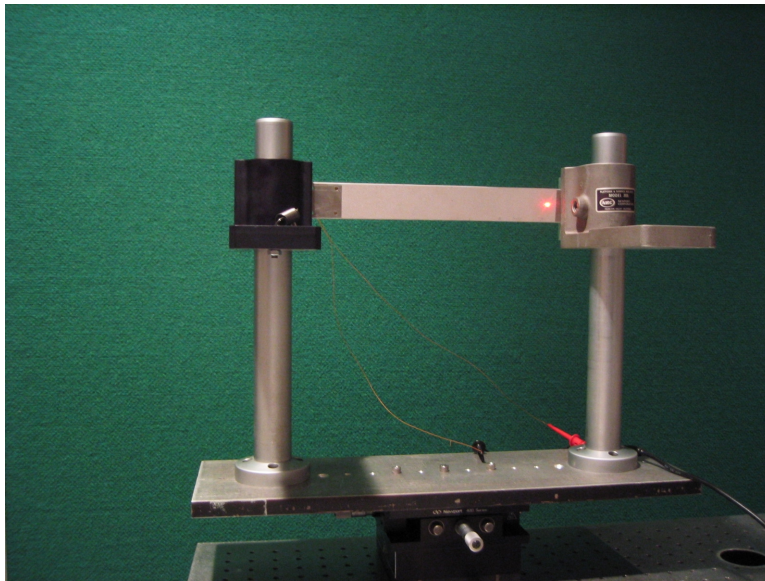


Figure B.1. Clamped-clamped beam fixed at both ends with a high reflectance diffuse coating. The clamped-clamped beam has a piezoelectric transducer used to excite it located on the back.



Figure B.2. Amplifier.



Figure B.3. Collimation Tester.



Figure B.4. Polytec OFV-3001 Controller(top) and Onisoki FFT Analyzer with Signal Generator(bottom).

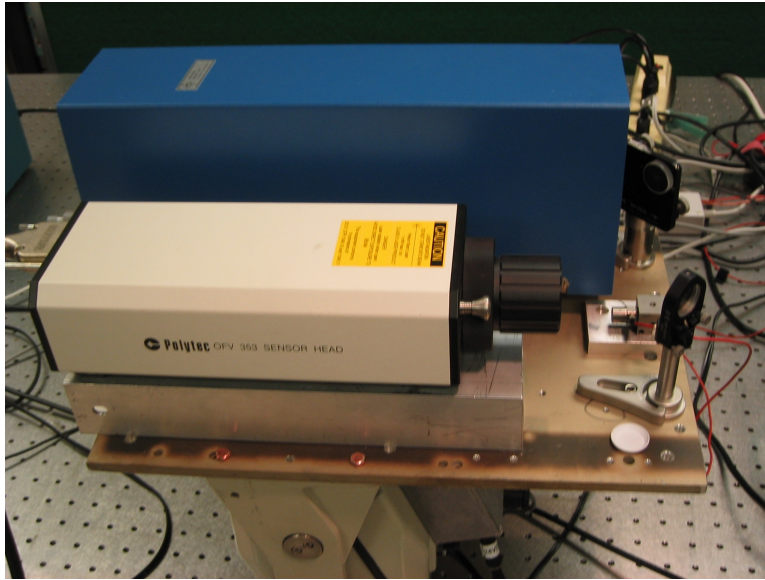


Figure B.5. Polytec Sensor Head OFV-353 and Beam Expander (Behind Sensor Head). The Laser Leaves the Sensor Head, gets reflected off two Mirrors into the Beam Expander. The Elevation and Azimuth of Directed Laser Energy is Controlled by Motors that Control the Plate on Which The Sensor Head and Beam Expander Sit. The Motors are Controlled by Laptop Software.

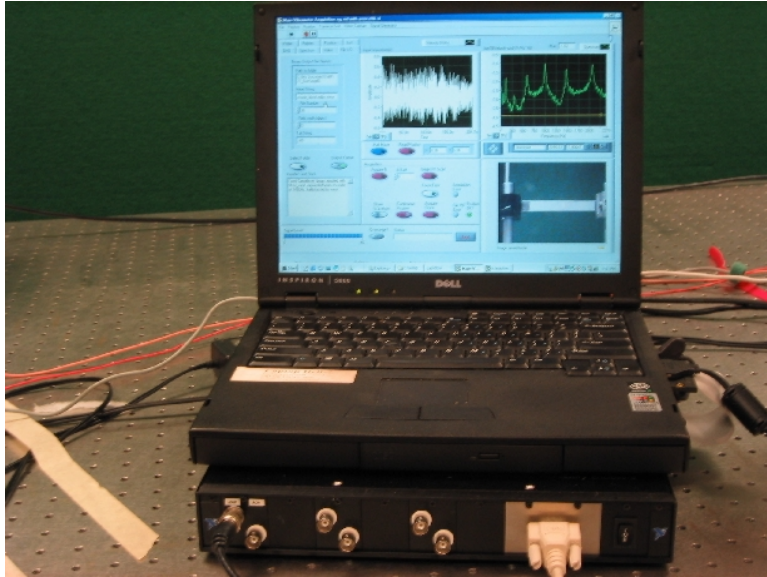


Figure B.6. Laptop Contains Software Developed by AFRL that Controls Both the Position of Directed Laser Energy and Records Information in File Format "1011" as is Shown in Appendix C.

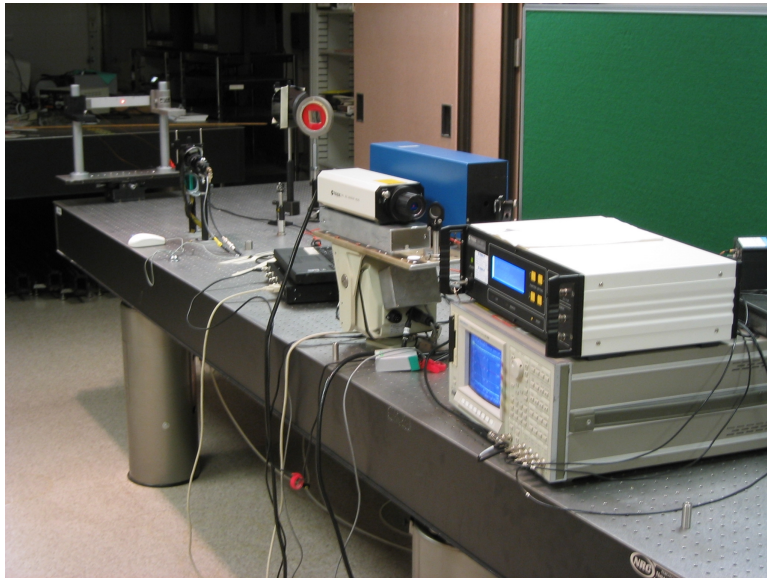


Figure B.7. Equipment Set Up to Take Readings.

Appendix C. File Format 1011 - AFRL (John Schmoll)

File Format Used to record data from LVS.

Main Header

Byte Order	U32
File Type	U32
Total Main Header Size in bytes	U32
Header string block size in bytes	U32
Variable Length header string	U32

Run Data

Total Block Size for this "run"	I32
Block size of following (U16)block^*	I32
Run Number	U16
N Channels of data	U16
Data Type	U16
Year	U16
Month	U16
Day	U16
Hour	U16
Minute	U16
Second	U16
Millisecond	U16
Microsecond	U16
Block size of following (SGL) block	I32
Velocity Range	SGL

Displacement Range	SGL
Track Filter	SGL
Low Pass Filter	SGL
Overrange	SGL
Position X	SGL
Position Y	SGL
Position Z	SGL

Waveform data (one waveform for each active channel)

For each Waveform{

block size of waveform in bytes	I32
Timestamp	DBL
Sample Interval(1/Sample Rate)	DBL
Number of samples of data in the following Waveform	
Data record	I32
Waveform Data	SGL

}

Appendix D. Modal Analysis - MATLAB® code

```
%readPolytech
%reads the polytech file (fname) from the path (temp) specified
%outputs avi file of PSD as a function of position for given freq
%
%Original Version (Mathew Dierking) AFRL - 2002
%
%Modified by N. Pepela - 12 December 2002
%Modifications added:
%Allow multiple wavelengths to be averaged
%Figures added to monitor PSD processing
%Converted to monitor Cantilever bar
%co-ordinate position of target converted to (px,py)
%2 bugs with reading in file corrected (file pointer bugs)

clear all;
pack;
fname= 'fixedcantilever15'; %filename
%directory
temp = ['C:\Student\Matlab\work\Thesis\Test Files\' ,fname, '.vib'];

%Set up constants
%%%%%%%%%%%%%%%%%%%%%%%%%%%%%%%%%%%%%%%%%%%%%%%%%%%%%%%%%%%%%%%%%%%%%%%%
Nfft=1024/2;%; %*4;%changes the fft 'window' size for averaging psd
NumberScanPoints = 525;%155; %33; %373; ;% % 33; %369% 368; %
cutFreq=5000; %5000; %1000; %650; %cutoff frequency for plot movie
No_waveforms = 10; % 10; % number of waveforms to average
```

```

px = zeros(1);
py = zeros(1);
pz = zeros(1);
%flag to plot monitoring figures. (1 = on,0=off)
figureon = 0;
%%%%%%%%%%%%%%%%%%%%%%%%%%%%%%%%%%%%%%%%%%%%%%%%%%%%%%%%%%%%%%%%%%%%%%%%

%open up file and read header information.This is for file type 1011
fid=fopen(temp);
byteorder = fread(fid,1,'uint32');
filetype = fread(fid,1,'uint32');
MHeaderSize = fread(fid,1,'uint32');
HeadStringSize = fread(fid,1,'uint32');
Header = fread(fid,HeadStringSize,'char');
for i=1:HeadStringSize;
    header(i)=sprintf('%c',Header(i));
end

Xavg=zeros(1,Nfft/2+1); %set up vectors to hold PSD
XX=zeros(10,Nfft/2+1);
XX=XX';

%Set up figures to plot all the scan points on the target
%figure(1);
fig=figure('Position',[550 75 500 400]); %1 500 200 200
clf;
%Double buffer helps have flash free figures
set(fig,'DoubleBuffer','on');

```

```

set(gca,'xlim',[-80 80],'ylim',[-80 80],'NextPlot',...
'replace','Visible','off');
avifname=sprintf('%s_%d.avi',fname,Nfft);
title('Plot of Scan Points');
colormap(hot);
if figureon == 1 %if figures turned on then set up figures

%figure(2);
fig=figure('Position',[200 500 450 250]);
title('Velocity mm/s');

%figure(3);
fig=figure('Position',[1 75 500 400]);
title('PSD of waveform');

%figure(4);
fig=figure('Position',[600 600 300 100]);

%figure(5);
fig=figure('Position',[550 75 500 400]);

end

mov = avifile(avifname);

%initialise counter
count = 1;

```

```

%read in the data info
for ix=1:NumberScanPoints*No_waveforms;
    %read in all settings
    RunBlk    = fread(fid,1,'int32');
    %if (RunBlk);
    BlkU16    = fread(fid,1,'int32');
    RunNo     = fread(fid,1,'ushort');
    nChan     = fread(fid,1,'ushort');
    DataType  = fread(fid,1,'ushort');
    Year      = fread(fid,1,'ushort');
    Month     = fread(fid,1,'ushort');
    Day       = fread(fid,1,'ushort');
    hour      = fread(fid,1,'ushort');
    minute    = fread(fid,1,'ushort');
    sec       = fread(fid,1,'ushort');
    msec      = fread(fid,1,'ushort');
    usec      = fread(fid,1,'ushort');
    SGLblk    = fread(fid,1,'int32');
    VelRng    = fread(fid,1,'float');
    DispRng   = fread(fid,1,'float');
    TrkFltr   = fread(fid,1,'float');
    LPF       = fread(fid,1,'float');
    SgnlLvl   = fread(fid,1,'float');
    OverRng   = fread(fid,1,'float');
    PosX      = fread(fid,1,'float');
    PosY      = fread(fid,1,'float');
    PosZ      = fread(fid,1,'float');

```

```

%calculate position of scan point
if count == No_waveforms
    b = ix/No_waveforms;
    px(b)=PosX;
    py(b)=PosY;
    pz(b)=PosZ;
end

if figureon == 1
    %plot scan point
    figure(1)
    plot(px,py,'+');drawnow;
end

for count = 1:No_waveforms

    %read in data record
    BlkWfm = fread(fid,1,'int32');
    %BlkWfm1 = fread(fid,1,'int');
    TimeStmp = fread(fid,1,'double');
    SampleInt= fread(fid,1,'double');
    Nsamples = fread(fid,1,'int32');

    %Wavefrm is the sampled velocity input
    Wavefrm = fread(fid,Nsamples,'float');
    Velocity = Wavefrm*VelRng; %scale to get velocity

    %Hanning window used of length Nfft

```

```

[Xavg,fx]=psd(Wavefrm,Nfft,1/SampleInt,Nfft,Nfft/2);

%display figures
if figureon == 1
    figure(2);
    plot(Velocity);
    title('velocity mm/s');
    %pause;
    figure(3);
    psdplot(Xavg,fx,'Hz','','PSD Plot');
    axis([0,cutFreq,-Inf,Inf]);

    figure(4);
    %fig=figure('Position',[500 500 400 100]);
    plot(fx,Xavg);
end

Xwav(:,count) = Xavg;

%display average PSD
if count == No_waveforms;
    matrixposn = ix/No_waveforms;
    XX(:,matrixposn) = (mean(Xwav,2));
    count = 0;
    if figureon ==1
        figure(5);
        psdplot(XX(:,ix/No_waveforms)',fx,'Hz','','...
        'PSD Average Plot');
    end
end

```



```

                axis([0,cutFreq,-Inf,Inf]);
            end
        end
        count = count+1;

end;

%close file
fclose(fid);

%transpose XX back
XX=XX';

%work out scaling factor.
gmax=max(max((XX(:,50:Nfft/2))));

%normalize max to 1
XS=XX/gmax;

%ilimit will give the position in vector XS and fx at
%which the frequency is at the cut-off frequency being examined
ilimit=cutFreq*SampleInt*Nfft+1;
if (ilimit > Nfft/2+1);
    ilimit=Nfft/2+1;
end

%for i=1:Nfft/2+1;

```

```

for i=2000:floor(ilimit); %for i=1:floor(ilimit);
    if(max(max(XS(:,i)))>.00001);%i;
        Ngrid=40;
        [xg,yg]=meshgrid(-3.1:.01:3.1,-.3:.01:.3); %cantilever
        [xg,yg,XSG]=griddata(px,py,XS(:,i),xg,yg,'cubic');
        image(flipud(XSG*150));
        axis image;
        temp=sprintf('%s, nfft = %d ,...
Frequency Bin %5.1f Hz',fname,Nfft,fx(i));
        title(temp);
        colorbar;
        F = getframe(gcf);           %grabs figure window
        mov = addframe(mov,F);
        %movietest(i) = F;
    end;
end
mov = close(mov); %close avi

```

Appendix E. Modeling of Clamped-Clamped Beam - MATLAB® Code

```
%Simulation of LVS on a canteliver beam.  
%N. Pepela - 17 December 2002.  
%Version 3  
  
%Assumptions:  
%Power in each eigenfrequency is the same.  
%each component along surface of illumination has equal intensity and  
%contribution towards LVS velocity signal.  
%No torsional mode effects.  
%start positions of phase are the same.  
%laser is perpendicular to beam.  
  
%changing number of modes requires 4 changes:  
%1. Update variable 'numberofmodes' (start of program)  
%2. Update displacement modes  
%3. Update illuminated displacement modes  
%4. Update illuminated velocity  
  
%buttons work - but not that well. Sometimes need to press a few  
%times to make work.  
  
%can increase laser width by playing with 'laserillum' variable  
%near start of program  
  
%Warnings produced by MATLAB have been examined and can be ignored
```

```

%lets begin
clear all; pack;
%lets inisialise some variables

%length and position of x(the surface) illuminated by laser - keep
%this same divisions as x (change width of laser - eg [.2:.01:.9])
laserillum = [.130:.001:.140];

numberofmodes = 6;    %total number of modes being modelled in beam
%time vector seconds - the divisions control the sampling freq and
%can hence affect aliasing if too low. speed of program compromised
%if too high.
t = [0:.0001:2.5];

t = t';
Vt = 0;                %initialise velocity of surface x

%yi contains the mode shapes that exist at the area the beam is
%illuminated
yi = zeros(6,length(laserillum));
%vi used to hold velocities of beam in laser illuminated area
vi = zeros(6,length(laserillum));
A = 1/numberofmodes;    %Amplitude
z = ones(1,101);        %vector so cantilever beam can be plotted in 3-d

```

```

%increase nfft will decrease bias of freq estimation .... but
%will take longer to determine frequency content
%length to which output velocity signal from LVS is zero padded before
%PSD is calculated
nfft = 256;%512; %1024; %256; 512; 1024;
ts = t(2) - t(1); %calculate sampling rate based on time vector
Fs = 1/ts; %sampling frequency
modeflag = zeros(1,10);

```

```

%%%%%%%%%%%%%%%%%%%%%%%%%%%%%%%%%%%%%%%%%%%%%%%%%%%%%%%%%%%%%%%%%%%%%%%%
%%Beam properties%%
%%%%%%%%%%%%%%%%%%%%%%%%%%%%%%%%%%%%%%%%%%%%%%%%%%%%%%%%%%%%%%%%%%%%%%%%

```

```

length_beam = .27;
%weighted frequencies as found in chap 3 of thesis
beta_1 = [4.73004074 7.85320462 10.9956079 14.1371655 17.2787597 ...
20.4203522];
beta=beta_1/length_beam;
%x is surface length of beam
x = [0:.001:length_beam];

%First six natural frequencies of beam calculated using
%Euler-Bernouli beam theory

```

```

%first six fundamental frequencies of beam
W = [112 308 605 1001 1495 2088];
%Mode-Shape Coefficient Calculation
sigma_ff_In = (cosh(beta_1) - cos(beta_1))./...
(sinh(beta_1) - sin(beta_1))

%y contains the different mode shapes that will
%exist in beam (6 is max number of modes)
y = zeros(6,length(x));

%%%%%%%%%%%%%%%%%%%%%%%%%%%%%%%%%%%%%%%%%%%%%%%%%%%%%%%%%%%%%%%%%%%%%%%%
%%screen properties%
%%%%%%%%%%%%%%%%%%%%%%%%%%%%%%%%%%%%%%%%%%%%%%%%%%%%%%%%%%%%%%%%%%%%%%%%

%Use screensize to set up figures
get(0,'ScreenSize'); set(0,'Units','normalized');

%set up some figures
%set up 2-d figure - contains the mode shapes
figure(2); clf; set(gcf,'Units','normalized');
set(gcf,'Position',[.015 .500 .300 .250]...
,'Color','k'); set(gca,'Position',[0.15 0.2 0.8 0.6]);
%axis([0 1 -1 1 -1 1]);

```

```

%voltage signal - emulates velocity signal given by LVS
figure(3); clf; set(gcf,'Units','normalized');
set(gcf,'Position', [.015 .050 .400...
.300],'Color','k'); set(gca,'Position',[0.15    0.2    0.8    0.6]);

% psd of voltage (velocity output of LVS) signal
figure(4); clf; set(gcf,'Units','normalized');
set(gcf,'Position', [.5 .1 .4
.3],'Color','k');

%set up 3-d animation of cantilever beam
fig = figure(1); clf; set(gcf,'Units','normalized');
set(gcf,'Position', [.3 .6 .7...
.3],'Color','k'); set(gca,'Position',[0.15    0.2    0.8    0.6]);

%buttons on fig 1
uicontrol('pos',[20 20 60 20],'string','done',...
'fontsize',8,'callback','close(gcf)');
uicontrol('pos',[20 40 60 20],'string','left',...
%set flag to -1 to indicate left button press
'fontsize',8,'callback','set(gcf,'userdata',-1)');
uicontrol('pos',[20 60 60 20],'string','right'...
%these buttons control laser illumination area
,'fontsize',8,'callback','set(gcf,'userdata',1)');
%this button to pause program
uicontrol('pos',[20 80 60 20],'string','Pause',...

```

```

'fontsize',8,'callback','set(gcf,'userdata',2)');

%set up Gaussian intensity profile of laser beam
%mean of Gaussian beam intensity profile
m = laserillum(length(laserillum)/2);
vari = 2; %variance of Gaussian beam intensity profile
gau = 15*(exp(- ((10.*(laserillum-m)).^2 / (2*vari)))) / ...
(vari * sqrt(2*pi));

%%%%%%%%%%%%%%%%%%%%%%%%%%%%%%%%%%%%%%%%%%%%%%%%%%%%%%%%%%%%%%%%%%%%%%%%
% main program   %%
%%%%%%%%%%%%%%%%%%%%%%%%%%%%%%%%%%%%%%%%%%%%%%%%%%%%%%%%%%%%%%%%%%%%%%%%

while ishandle(fig)
    for count = 1:length(t)

        %first check if button has been pressed to update
        %laser illuminated area
        checkbutton = get(fig,'userdata');
        if checkbutton == -1
            %shift laser illumination area left
            laserillum = laserillum - .001;

```



```

        set(fig,'userdata',0);
elseif checkbutton == 1
        laserillum = laserillum +.001;
        set(fig,'userdata',0);
end

%lets do some modeling
%%%%%%%%displacement Modes%%%%%%%%
%enter mode shapes - max 10

%experiment
%first plot mode shapes for clamped- clamped

%mode shape using inman
%A is used to normalize according to number of
%modes present

y(1,:) = (cosh(beta(1)*x) - cos(beta(1)*x) - ...
(sigma_ff_In(1)*(sinh(beta(1)*x) - sin(beta(1)*x))))...
* cos(2*pi*W(1)*t(count));
y(2,:) = (cosh(beta(2)*x) - cos(beta(2)*x) - ...
(sigma_ff_In(2)*(sinh(beta(2)*x) - sin(beta(2)*x))))...
* cos(2*pi*W(2)*t(count));
y(3,:) = (cosh(beta(3)*x) - cos(beta(3)*x) - ...
(sigma_ff_In(3)*(sinh(beta(3)*x) - sin(beta(3)*x))))...
* cos(2*pi*W(3)*t(count));
y(4,:) = (cosh(beta(4)*x) - cos(beta(4)*x) - ...

```

```

(sigma_ff_In(4)*(sinh(beta(4)*x) - sin(beta(4)*x)))...
* cos(2*pi*W(4)*t(count));
y(5,:) = (cosh(beta(5)*x) - cos(beta(5)*x) - ...
(sigma_ff_In(5)*(sinh(beta(5)*x) - sin(beta(5)*x)))...
* cos(2*pi*W(5)*t(count)));
y(6,:) = (cosh(beta(6)*x) - cos(beta(6)*x) - ...
(sigma_ff_In(6)*(sinh(beta(6)*x) - sin(beta(6)*x)))...
* cos(2*pi*W(6)*t(count)));

%normalize to 1 by dividing by gmax, and normalize
%depending on # of modes by mult by A
if count == 1
    for i = 1:6
        gmax(i) = max(abs(y(i,:)));
    end
end

for i = 1:6
    if gmax(i) > 0
        y(i,:) = y(i,:)*A/gmax(i);
    end
end

%calculate sum of all modes
yt = sum(y);

```

```

%%%%%%%%%Illuminated displacement Modes%%%%%%%%%
%calculate the instantaneous displacement due at the
%illuminated area.

yi(1,:) = (cosh(beta(1)*laserillum) - cos(beta(1)*...
laserillum) - (sigma_ff_In(1)*(sinh(beta(1)*laserillum)...
- sin(beta(1)*laserillum)))) * cos(2*pi*W(1)*t(count));
yi(2,:) = (cosh(beta(2)*laserillum) - cos(beta(2)*...
laserillum) - (sigma_ff_In(2)*(sinh(beta(2)*laserillum)...
- sin(beta(2)*laserillum)))) * cos(2*pi*W(2)*t(count));
yi(3,:) = (cosh(beta(3)*laserillum) - cos(beta(3)*...
laserillum) - (sigma_ff_In(3)*(sinh(beta(3)*laserillum)...
- sin(beta(3)*laserillum)))) * cos(2*pi*W(3)*t(count));
yi(4,:) = (cosh(beta(4)*laserillum) - cos(beta(4)*...
laserillum) - (sigma_ff_In(4)*(sinh(beta(4)*laserillum)...
- sin(beta(4)*laserillum)))) * cos(2*pi*W(4)*t(count));
yi(5,:) = (cosh(beta(5)*laserillum) - cos(beta(5)*...
laserillum) - (sigma_ff_In(5)*(sinh(beta(5)*laserillum)...
- sin(beta(5)*laserillum)))) * cos(2*pi*W(5)*t(count));
yi(6,:) = (cosh(beta(6)*laserillum) - cos(beta(6)*...
laserillum) - (sigma_ff_In(6)*(sinh(beta(6)*laserillum)...
- sin(beta(6)*laserillum)))) * cos(2*pi*W(6)*t(count));

%normalize to 1 by dividing by gmax, and normalize depending
%on # of modes by mult by A

for i = 1:6

```

```

    if gmax(i) > 0
        yi(i,:) = yi(i, :)*A/gmax(i);
    end
end

%sum of all displacements
yti = sum(yi);

%%%%%%%%%Illuminated velocity%%%%%%%%%
%calculate velocities :derivatives of the displacement
%with respect to time
vi(1,:) = (cosh(beta(1)*laserillum) - cos(beta(1)*...
laserillum) - (sigma_ff_In(1)*(sinh(beta(1)*...
laserillum) - sin(beta(1)*laserillum)))) * ...
-2*pi*W(1)*sin(2*pi*W(1)*t(count));
vi(2,:) = (cosh(beta(2)*laserillum) - cos(beta(2)*...
laserillum) - (sigma_ff_In(2)*(sinh(beta(2)*...
laserillum) - sin(beta(2)*laserillum)))) * ...
-2*pi*W(2)*sin(2*pi*W(2)*t(count));
vi(3,:) = (cosh(beta(3)*laserillum) - cos(beta(3)*...
laserillum) - (sigma_ff_In(3)*(sinh(beta(3)*...
laserillum) - sin(beta(3)*laserillum)))) * ...
-2*pi*W(3)*sin(2*pi*W(3)*t(count));
vi(4,:) = (cosh(beta(4)*laserillum) - cos(beta(4)*...
laserillum) - (sigma_ff_In(4)*(sinh(beta(4)...
*laserillum) - sin(beta(4)*laserillum)))) * ...
-2*pi*W(4)*sin(2*pi*W(4)*t(count));

```

```

vi(5,:) = (cosh(beta(5)*laserillum) - cos(beta(5)*...
laserillum) - (sigma_ff_In(5)*(sinh(beta(5)...
*laserillum) - sin(beta(5)*laserillum)))) * ...
-2*pi*W(5)*sin(2*pi*W(5)*t(count));
vi(6,:) = (cosh(beta(6)*laserillum) - cos(beta(6)*...
laserillum) - (sigma_ff_In(6)*(sinh(beta(6)...
*laserillum) - sin(beta(6)*laserillum)))) * ...
-2*pi*W(6)*sin(2*pi*W(6)*t(count));

```

```

%Vt will give sum of all velocity components along the
%illuminated surface

```

```

Vt = sum((sum(vi)).*gau);

```

```

%This vector contains all velocities due to surface over time
V(count,:) = Vt;

```

```

%set flags to determine which modes exist -
%this will assist in plotting mode shapes in fig(2)
if count == 1
    for i = 1:6;
        nonzeromode = (find(abs(y(i,:)))>0);
        if nonzeromode > 0
            modeflag(i) = 1;
        end
    end
end

```

```

        end
    end
end

%%%%%%%%%%%%%%%%%%%%%%%%%%%%%%%%%%%%%%%%%%%%%%%%%%%%%%%%%%%%%%%%%%%%%%%%start plots here%%%%%%%%%%%%%%%%%%%%%%%%%%%%%%%%%%%%%%%%%%%%%%%%%%%%%%%%%%%%%%%%%%%%%%%%
%plot 3-d - current position of cantilever
figure(1);
w = z'*yt;    %w to plot canteliver in 3-d
set(gca,'Color','k','Xcolor','w','Ycolor','w','Zcolor','w');
c = w;
%find start position of laser illumination on canteliver
px = find(x > laserillum(1));
%area illuminated by cantilever
c(:,(px(1)-1):(px(1)-1+length(laserillum))) = 1.01;
surf(w,c);    %plot cantilever with laser beam
set(gca,'CameraUpVector',[0 0 1],'View',[1.5 82],...
'Projection','perspective');
axis([0 length(x) -200 200 -2 2]);
axis off
set(gca,'Color','k','Xcolor','w','Ycolor','w',...
'Zcolor','w');
text(0,-100,0,['Instantaneous Velocity Due to ...
illum area = ',num2str(Vt),'m/s'],'FontSize',...
10,'Color','w');
text(0,-150,0,['time = ',num2str(t(count)),'s']...
,'FontSize',10,'Color','w');

```

```

text(0,-200,0,['illum area =',num2str...
(laserillum(1)),' - ',num2str(laserillum(length...
(laserillum)))],'FontSize',10,'Color','w');
title(['.27m Clamped-Clamped Beam - Illuminated ...
by LVS'],'Color','w');
shading interp;
cmap = [copper(255); 1 .1 .1];
colormap(cmap);

%plot all mode shapes in figure(2) - assume max
%number of modes is 6
for i = 1:6
    figure(2);
    %this loop will prevent us from plotting
    %any zero modes
    if modeflag(i) == 1
        plot(x,y(i,:), 'c');
        axis([0 length_beam -1.1 1.1]);
        axis on;
        hold on;
    end
end

%plot sum of all modes shape in figure 2
plot(x,yt, 'b', 'LineWidth', 2);
set(gca, 'Color', 'k', 'Xcolor', 'w', 'Ycolor', 'w');
xlabel('Length of Beam (m)', 'Color', 'w');
ylabel('Space', 'Color', 'w');

```

```

title(['Spatial sum of modes vibrating on Beam']...
,'Color','w');
%plot laserilluminated area
plot(laserillum,yti,'r','LineWidth',1);
%set(gca,'CameraPosition',[0 0 0]);
hold off

%display current velocity signal

%plot(t(1:count),V,'g');
if count > 1
    figure(3);
    %plots voltage against currently collected data
    plot(t(count-1:count),V(count-1:count),'b','...
    LineWidth',2);
    set(gca,'Color','k','Xcolor','w','Ycolor','w');
    xlabel('time (s)','Color','w');
    ylabel('Velocity','Color','w');
    title(['Velocity output from LVS due to illuminated ...
    area'],'Color','w');
    hold on;
end

%calculate PSD due to current sampled total
%voltage and plot
figure(4);
%set up velocity to take PSD of last nfft

```



```

%sampled points of signal
if length(V) <= nfft
    Vps = V;
else
    Vps(1) = [];
    Vps = [Vps ; V(length(V))];
end

%hanning window of size nfft is used
[Pxx,fx]=psd(Vps,nfft,Fs,nfft,(nfft/2));
psdplot(1000*Pxx,fx,'Hz');
set(gca,'Color','k','Xcolor','w','Ycolor',...
'w','Xlim',[0 2500]);

%pause button control
checkboxbutton = get(fig,'userdata');
if checkboxbutton == 2
    pause;
    set(fig,'userdata',0);
end
drawnow;
%pause;

end
end

```

```

%fixes/changes in Version 3 from previous version
%Now uses Gaussian beam to illuminate target
%Target is .27m fixed-fixed beam

```

Bibliography

1. Acherekar, M., et al. "Laser Vibration Sensor," *Infrared Technology XIV, SPIE - vol. 2472*:2–11 (1995).
2. Brehmer, A. "Normal Mode Testing Using A Scanning Laser Doppler Vibrometer," *Proceedings of SPIE: Third International Conference on Vibration Measurement by Laser Techniques:Advances and Applications, 4072*:184–193 (2000).
3. Bucher, I. "Measuring Vibration Spatial Using Continuous Laser Scanning," *Proceedings of SPIE: Third International Conference on Vibration Measurement by Laser Techniques:Advances and Applications, 3411*:409–417 (1998).
4. Castellini, P., et al. "Tracking Laser Doppler Vibrometer for Linear Motion: Application to a Timing Belt," *Proceedings of SPIE: Third International Conference on Vibration Measurement by Laser Techniques:Advances and Applications, 4072*:194–200 (2000).
5. Chen, S., et al. "Damage Detection Using Scanning Laser Vibrometer," *Third International Conference on Vibration Measurements by Laser Techniques: Advances and Applications, SPIE - vol. 3411*:473–484 (1998).
6. Drain, L.E. *The Laser Doppler Technique*. New York: John Wiley & Sons Ltd, 1980.
7. F., Buell W., et al. "Bayesian Spectrum Analysis for Laser Vibrometry Processing," *Institute for Advanced Physics*
8. Gade, S., et al. "Modal Analysis Using a Scanning Laser Doppler Vibrometer," *Proceedings of IMAC-XX: A Conference on Structural Dynamics, SPIE - vol. 4753*:1015–1019 (2002).
9. Gasper, J.L., et al. "Membrane Vibration Studies Using a Scanning Laser Vibrometer," *Proceedings of IMAC-XX: A Conference on Structural Dynamics, SPIE - vol. 4753*:1532–1538 (2002).
10. Hamming, R.W. *Numerical Methods for Scientists and Engineers, 2nd Ed.* Ontario: Dover Publications, 1973.
11. Hecht, E. *Optics*. San Francisco: Addison Wesley, 2002.
12. Hlawatsch, F. *Time-Frequency Analysis and Synthesis of Linear Signal Spaces*. United States: Kluwer Academic Publishers, 1998.
13. Inman, D.J. *Engineering Vibration*. Upper Saddle River New Jersey: Prentice Hall, 1996.
14. J.W., Goodman. *Introduction to Fourier Optics*. Boston: McGraw-Hill, Inc, 1996.

15. Kachelmyer, A. L., et al. "Ship Identification by Coherent LADAR Vibration Sensing," *IRIS Active Systems*, vol. 1:379–398 (1992).
16. Kay, S. M. *Modern Spectral Estimation*. United States: Prentice Hall, 1988.
17. Kranz, W. "Target Classification by Vibration Sensing," *Infrared Technology XIV, SPIE - vol. 972:383–387* (1988).
18. Larson, R.E. and B.H. Edwards. *Elementary Linear Algebra*. United States: D.C. Heath and Company, 1991.
19. Meirovitch, L. *Elements of Vibrational Analysis*. Mexico: McGraw-Hill, Inc, 1986.
20. Mullis, C.T. and R.A. Roberts. *Digital Signal Processing*. United States: Addison-Wesley, 1987.
21. Newland, D. E. *Random Vibrations, Spectral Analysis and Wavelet Analysis*. New York: John Wiley & Sons, 1993.
22. Pinotti, M., et al. "Cartoid Artery Pulse Wave Measured by a Laser Vibrometer," *Third International Conference on Vibration Measurements by Laser Techniques: Advances and Applications, SPIE - vol. 3411:611–616* (July 1998).
23. Polytech. "Laser Doppler Vibrometer User Manual." User Manual, no date [2000].
24. Polytech. "Vibrometer University - Laser Vibrometer Basics." <http://www.polytec.de/cgi-bin/clickgo.cgi>, December 2002.
25. Russell, D. "Acoustics and Vibration Animations." <http://www.kettering.edu/~drussell/Demos/string/Fixed.html>, December 2002.
26. Scharf, L.L. *Statistical Signal Processing*. United States: Addison-Wesley, 1991.
27. Shanmugan, K.S. and A.M. Breippohl. *Random Signals: Detection, Estimation and Data Analysis*. New York: John Wiley & Sons, 1988.
28. Stanbridge, A.B., et al. "Modal Testing Using Impact Excitation and a Scanning LDV," *Third International Conference on Vibration Measurements by Laser Techniques: Advances and Applications, SPIE - vol. 3411:348–356* (1998).
29. Stanbridge, A.B., et al. "Continuous-Scan Vibration Measurements on Moving Components," *Proceedings of IMAC-XX: A Conference on Structural Dynamics, SPIE - vol. 4753:1519–1525* (2002).
30. Streat, R.F., et al. "Global Noise Characteristics of a Laser Doppler Vibrometer Part I: Theory," *Vibration Measurements by Laser Techniques: Advances and Applications*, vol. 2868:2–11 (1996).

31. Tomasini, E. P. "Second International Conference on Vibration Measurements by Laser Techniques: Advances and Applications," *SPIE - The International Society for Optical Engineering*, vol. 2868(4):745-808 (July 1996).
32. Verdeyen, J.T. *Laser Electronics*. Upper Saddle River, New Jersey: Prentice Hall, 1995.

REPORT DOCUMENTATION PAGE			Form Approved OMB No. 074-0188		
<p>The public reporting burden for this collection of information is estimated to average 1 hour per response, including the time for reviewing instructions, searching existing data sources, gathering and maintaining the data needed, and completing and reviewing the collection of information. Send comments regarding this burden estimate or any other aspect of the collection of information, including suggestions for reducing this burden to Department of Defense, Washington Headquarters Services, Directorate for Information Operations and Reports (0704-0188), 1215 Jefferson Davis Highway, Suite 1204, Arlington, VA 22202-4302. Respondents should be aware that notwithstanding any other provision of law, no person shall be subject to a penalty for failing to comply with a collection of information if it does not display a currently valid OMB control number.</p> <p>PLEASE DO NOT RETURN YOUR FORM TO THE ABOVE ADDRESS.</p>					
1. REPORT DATE (DD-MM-YYYY) 23-03-2002		2. REPORT TYPE Master's Thesis		3. DATES COVERED (From – To) Jun 2002 – Mar 2003	
4. TITLE AND SUBTITLE EFFECT OF MULTI-MODE VIBRATION ON SIGNATURE ESTIMATION USING A LASER VIBRATION SENSOR			5a. CONTRACT NUMBER		
			5b. GRANT NUMBER		
			5c. PROGRAM ELEMENT NUMBER		
6. AUTHOR(S) Pepela, Ngoya, Flight Lieutenant, Royal Australian Air Force			5d. PROJECT NUMBER		
			5e. TASK NUMBER		
			5f. WORK UNIT NUMBER		
7. PERFORMING ORGANIZATION NAMES(S) AND ADDRESS(S) Air Force Institute of Technology Graduate School of Engineering and Management (AFIT/EN) 2950 Hobson Way, Building 640 WPAFB OH 45433-7765			8. PERFORMING ORGANIZATION REPORT NUMBER AFIT/GE/ENP/03-02		
9. SPONSORING/MONITORING AGENCY NAME(S) AND ADDRESS(ES) AFRL Attn: Mr. Matthew Dierking 1865 4 th Street WPAFB OH 45433-7765 PH: (937)-255-9614			10. SPONSOR/MONITOR'S ACRONYM(S)		
			11. SPONSOR/MONITOR'S REPORT NUMBER(S)		
12. DISTRIBUTION/AVAILABILITY STATEMENT APPROVED FOR PUBLIC RELEASE; DISTRIBUTION UNLIMITED.					
13. SUPPLEMENTARY NOTES					
14. ABSTRACT A laser vibration sensor (LVS) can be used to determine the vibrational spectrum of targets such as vehicles using heterodyne laser doppler velocimetry. The vibrational spectra of exterior skin of vehicles are known to have characteristic resonances due to the physical structure driven by motors, gears and other moving parts. Each particular class of vehicle has a unique vibrational spectrum. This research shows how a body vibrating in higher order modes has the opportunity to eliminate spectral content of the target's vibrational spectrum while using an LVS to perform spectrum estimation. This is due to roughly equal amounts of laser photons with equal and opposite information about the target's vibrational velocity returning from the body under investigation. This is especially so when observing targets at large distances, and the laser spot size has increased to encapsulate higher order modes vibrating at frequencies used for identification purposes. The research also contains preliminary investigations into the mitigation of these effects by use of laser scanning, laser pattern intensity changing and advanced signal processing techniques.					
15. SUBJECT TERMS Laser Doppler Vibrometer, Laser Vibration Sensor, Laser Vibrations Sensor, Vibrometer, Multi-Mode, Signature Estimation					
16. SECURITY CLASSIFICATION OF:		17. LIMITATION OF ABSTRACT	18. NUMBER OF PAGES	19a. NAME OF RESPONSIBLE PERSON	
a. REPORT	b. ABSTRACT			c. THIS PAGE	Marciniak, Michael A. Lt Col, USAF (ENP)
U	U	UU	92	19b. TELEPHONE NUMBER (Include area code) (937) 255-3636, ext 4529; e-mail: Michael.Marciniak@afit.edu	

Standard Form 298 (Rev. 8-98)
Prescribed by ANSI Std. Z39-18